The di-photon excess in a perturbative SUSY model

Karim Benakli, Luc D Darmé, Mark D. Goodsell, Julia Harz

Available online at www.sciencedirect.com

ScienceDirect

Nuclear Physics B 911 (2016) 127–162

NUCLEAR PHYSICS B

www.elsevier.com/locate/nuclphysb

The di-photon excess in a perturbative SUSY model

Karim Benakli [a,b], Luc Darmé [a,b,c], Mark D. Goodsell [a,b], Julia Harz [a,b,c,*]

[a] *Sorbonne Universités, UPMC Univ Paris 06, UMR 7589, LPTHE, F-75005, Paris, France*
[b] *CNRS, UMR 7589, LPTHE, F-75005, Paris, France*
[c] *Sorbonne Universités, Institut Lagrange de Paris (ILP), 98 bis Boulevard Arago, 75014 Paris, France*

Received 18 June 2016; received in revised form 22 July 2016; accepted 23 July 2016

Available online 28 July 2016

Editor: Tommy Ohlsson

Abstract

We show that a 750 GeV di-photon excess as reported by the ATLAS and CMS experiments can be reproduced by the Minimal Dirac Gaugino Supersymmetric Standard Model (MDGSSM) without the need of any ad-hoc addition of new states. The scalar resonance is identified with the spin-0 partner of the Dirac bino. We perform a thorough analysis of constraints coming from the mixing of the scalar with the Higgs boson, the stability of the vacuum and the requirement of perturbativity of the couplings up to very high energy scales. We exhibit examples of regions of the parameter space that respect all the constraints while reproducing the excess. We point out how trilinear couplings that are expected to arise in supersymmetry-breaking mediation scenarios, but were ignored in the previous literature on the subject, play an important role.

1. Introduction

In the first presentation of LHC Run 2 data, both experiments ATLAS and CMS presented an excess in the di-photon mass spectrum for comparable invariant masses. The CMS analysis observed its largest excess in the di-photon mass spectrum based on 2.6 fb^{-1} of pp collisions at

* Corresponding author.
E-mail addresses: kbenakli@lpthe.jussieu.fr (K. Benakli), darme@lpthe.jussieu.fr (L. Darmé), goodsell@lpthe.jussieu.fr (M.D. Goodsell), jharz@lpthe.jussieu.fr (J. Harz).

http://dx.doi.org/10.1016/j.nuclphysb.2016.07.027

$\sqrt{s} = 13$ TeV for an invariant mass of 760 GeV with a local significance of 2.6 σ and a global significance of smaller than 1.2 σ [1]. Similarly, the ATLAS collaboration reported the largest deviation from the background hypothesis for an invariant mass of 750 GeV using 3.2 fb^{-1} of data, leading to a local significance of 3.6 σ and a global significance of 2.0 σ taking into account the look-elsewhere-effect in the mass range of $m_{\gamma\gamma} \in [200\text{–}2000]$ GeV [2].

After updating and refining their analysis, CMS achieved an improved sensitivity by more than 20% and added a new data set which was taken with $B = 0$ T reaching as well a comparable 3.3 fb^{-1}. The modest excess at 750 GeV for the combined 8 and 13 TeV data remained with 3.4 σ (local) and 1.6 σ (global) significance [3]. ATLAS updated their 8 TeV analysis and confirmed the modest excess at 750 GeV in the Run I data set with a significance of 1.9 σ. Thus, the recent updates strengthen the hint for a new physics signal.

For the Spin-0 hypothesis and under the assumption of $\Gamma/m_\Phi = 0.014 \times 10^{-2}$ (with m_Φ the scalar singlet mass) the combined dataset of CMS with 3.3 fb^{-1} (13 TeV) and 19.7 fb^{-1} (8 TeV) gives the production cross-section times branching ratio into two photons to be

$$\sigma^{13\text{ TeV}} \cdot B_{\gamma\gamma} \approx 3.7 \pm 2 \text{ fb}, \tag{1.1}$$

while one analysis of the ATLAS data gives [4]

$$\sigma^{13\text{ TeV}} \cdot B_{\gamma\gamma} \approx 12 \pm 2 \text{ fb}. \tag{1.2}$$

An interpretation of this excess is that it is due to the production and subsequent decay of a scalar resonance of mass 750 GeV; while there have been many alternatives proposed (too many to mention here), we shall restrict to that case here as the most obvious and least tuned option in perturbative theories. The existence of such a particle with a mass close to the electroweak scale implies a new hierarchy problem that cannot obviously have an anthropic explanation, and this naturally strengthens the case for low-energy supersymmetry. However, the observed rate of diphoton production via the resonance is too large compared to what is expected from a heavy Higgs companion of the light Standard Model (SM)-like one, and in particular it is very difficult to justify in the Minimal Supersymmetric Standard Model (MSSM) (see e.g. [5–7][1]). In fact, the interpretation of the excess is challenging for most previously proposed supersymmetric extensions of the Standard Model, and of the perturbative models proposed since the announcement almost all invoke additional vector-like fermions and/or bosons. For an early review see [11]. In this work we shall show, on the other hand, that a previously proposed supersymmetric extension of the Standard Model called the Minimal Dirac Gaugino Supersymmetric Standard Model (MDGSSM) [12] contains all of the ingredients to explain the excess.

Since the proposal in [13] of extending the MSSM with extra states in the adjoint representation of the Standard Model to allow Dirac gaugino masses, this possibility has been subject to many studies due to their theoretical and phenomenological advantages: they allow simpler models of supersymmetry-breaking due to preserving an R-symmetry; their masses are supersoft [14] and supersafe from collider searches [15–17]; they ameliorate the SUSY flavour problem [18–20]; and contain new couplings which aid the naturalness of the Higgs mass [12,21–26]. Indeed, multiple realisations have been proposed that differ by the fate of R-symmetry, the presence or absence of additional states and interactions [14,22–24,27–63] (for a short introduction

[1] Note that although there have been several attempts to fit the excess in just the MSSM, such as in [8,9], they require a large fine-tuning of masses/parameters to be on resonance, and even then there remain questions about the viability of the scenario from e.g. vacuum stability constraints. In [10] it is unlikely that the enhancement of the chargino loop is valid once the width of the singlet is taken into account.

see for example [64]). Here we consider the case of the MDGSSM which was introduced with a minimal content of extra states to automatically preserve unification of gauge couplings while allowing the new couplings to the Higgs to enhance naturalness and allow the boundary conditions to be unified at a high energy scale.

We will show that it is one of the most promising models when it comes to reproduce the diphoton excess. Without any ad-hoc addition, all the necessary ingredients are already present in the MDGSSM:

- There is a singlet supermultiplet **S** introduced to give the Bino a Dirac gaugino mass. It is straightforward to identify its scalar (or pseudoscalar) component with the 750 GeV resonance.
- There are extra vector-like charged states, subsequently called "fake leptons" [65] as they carry the same quantum numbers as the Standard Model leptons. They were introduced in order to restore the automatic gauge coupling unification that was spoiled by the addition of the adjoint representations of the Standard Model gauge group. In this work, these states will increase the coupling of the scalar resonance to photons at one loop.
- There is an octet supermultiplet **O** required to give the gluino a Dirac mass. This contains colour-octet scalars which will generate a coupling of the singlet resonance to gluons at one loop (via trilinear scalar couplings), required for its production in gluon fusion.

One of the important constraints to impose on any new scalar S candidate to explain the excess is a bound on its mixing with the Standard Model Higgs. This mixing is not only induced at one-loop, but can be present already at tree level. The supersymmetric operator describing the Dirac gaugino bino mass leads to a modification of the $U(1)_Y$ D-term as

$$D_1 = D_Y^{(0)} \to D_1 = -2m_{1D} S_R + D_Y^{(0)} \qquad \text{with} \qquad D_Y^{(0)} = -g' \sum_j Y_j \varphi_j^* \varphi_j \tag{1.3}$$

where S_R is the real part of S and φ_j a scalar field with charge Y_j under $U(1)_Y$. Upon elimination of the auxilliary fields, this implies an interaction of the form:

$$g' m_{1D} S_R (|H_u^0|^2 - |H_d^0|^2), \tag{1.4}$$

thereof a tree-level induced mixing. However, this is typically compensated by the presence in the superpotential of a term of the form:

$$W \supset \lambda_S S H_u H_d. \tag{1.5}$$

A precise evaluation of this mixing at the tree and one-loop level needs to be carried out carefully if one tries to identify the scalar S in models of Dirac gauginos with a 750 GeV resonance.

Our parameter space is constrained by the requirements of stability of the vacuum avoiding existence of directions in the phase space of the model taking the fields expectation values to charge- and colour-breaking vacua. This is important as we shall see that trilinear terms will play an important role in generating the required amount of scalar production and decay into di-photons. Among the trilinear terms considered here some have not been explicitly discussed in the existing literature while they are expected to be generically present in the model. This is the case for example of soft terms mixing three adjoint scalars that we will show that they are generated in models of gauge mediation.

We shall keep couplings small enough to preserve perturbativity up to the GUT scale. This restriction can be of course relaxed if one allows for Landau poles below the GUT scale. However,

as one of the virtues of the MSSM was to predict perturbative unification of gauge couplings, and was one of the motivations for introducing the MDGSSM, we shall place emphasis on finding regions of the parameter space which respect this condition.

To find the parameter space relevant for the diphoton excess we shall use the most sophisticated tool available: the code SARAH [66–71] and its SPheno [72,73] output. This is able to calculate the masses of all particles to full one-loop order, and two-loops in the gaugeless limit for the neutral (pseudo)scalars [74–76]. It can calculate renormalisation group equations of all couplings to two-loop order, including the masses and tadpoles in Dirac gaugino models as given in [77]. A guide to its use for studying the diphoton excess was described in [11]; we make some small modifications described in section 5.1. In particular, this will allow us to obtain the production and decays of our resonance at 8 and 13 TeV while simultaneously accurately computing its mass and assuring that the light Higgs mass is correct, and verifying that the mixing between the singlet and the Higgs is small (also computed at two loops). We shall find that quantum corrections to the spectrum of particles are not just important but essential for understanding how the model describes the excess.

Finally, we note that there have been three previous attempts to relate models with Dirac gaugino masses with the diphoton excess. In [78] as in this work the scalar component of S was the putative resonance; however, the entire coupling was driven by (1.4) which required very large Dirac gaugino masses (which would potentially flatten the Higgs potential). In [79] the candidate is a neutral component of a scalar doublet R_u^0 introduced in the MRSSM to preserve R-symmetry, but the model required the R-symmetry to be broken to fit the excess and the Dirac nature of the gauginos played little role. As we were preparing to submit this work, [80] appeared, where the pseudoscalar component of S plays the role of the resonance; it couples entirely via superpotential couplings to coloured and charged fermions and thus requires large Majorana gaugino masses and charginos close to the threshold of 375 GeV to generate the couplings to photons and gluons. Here we will not require Majorana masses,[2] and will include only ingredients already allowed in the MDGSSM.

The paper is organised as follows. In section 2, we summarise the MDGSSM field content and interactions. To generate a large gluon coupling we require trilinear scalar adjoint couplings, the generation of which we describe in section 3 along with some observations on adjoint scalar masses. We discuss the constraints on the model in section 4; in particular, this includes a detailed study of vacuum stability, and an analysis of the constraints on colour octet scalars which are important and interesting in the context of this model. Our numerical results are provided in section 5: we consider four different scenarios which vary depending on the origin of R-symmetry violation, and give benchmark points to illustrate how our model reproduces the signal. Our results are summarised in the conclusions.

2. The minimal Dirac gaugino model

2.1. Model content and Lagrangian

In this section we review the main ingredients of the Minimal Dirac Gaugino Supersymmetric Standard Model (MDGSSM) introduced in [12].

[2] Except for our final scenario, which contains a double peak structure that can mimic a large width resonance – as discussed in e.g. [81–84].

Table 1
Chiral and gauge multiplet fields in the model.

Names		Spin 0	Spin 1/2	Spin 1	$(SU(3), SU(2), U(1)_Y)$	R-charge
Quarks	$\mathbf{Q}$	$\tilde{Q} = (\tilde{u}_L, \tilde{d}_L)$	(u_L, d_L)		$(\mathbf{3}, \mathbf{2}, 1/6)$	1
	$\mathbf{U^c}$	$\tilde{U}^c_L$	U^c_L		$(\overline{\mathbf{3}}, \mathbf{1}, -2/3)$	0
(×3 families)	$\mathbf{D^c}$	$\tilde{D}^c_L$	D^c_L		$(\overline{\mathbf{3}}, \mathbf{1}, 1/3)$	0
Leptons	$\mathbf{L}$	$(\tilde{\nu}_{eL}, \tilde{e}_L)$	(ν_{eL}, e_L)		$(\mathbf{1}, \mathbf{2}, -1/2)$	1
(×3 families)	$\mathbf{E^c}$	$\tilde{E}^c$	E^c		$(\mathbf{1}, \mathbf{1}, 1)$	0
Higgs	$\mathbf{H_u}$	(H^+_u, H^0_u)	$(\tilde{H}^+_u, \tilde{H}^0_u)$		$(\mathbf{1}, \mathbf{2}, 1/2)$	1
	$\mathbf{H_d}$	(H^0_d, H^-_d)	$(\tilde{H}^0_d, \tilde{H}^-_d)$		$(\mathbf{1}, \mathbf{2}, -1/2)$	1
Gluons	$\mathbf{W_{3\alpha}}$		$\lambda_{3\alpha}$ $[\equiv \tilde{g}_\alpha]$	g	$(\mathbf{8}, \mathbf{1}, 0)$	1
W	$\mathbf{W_{2\alpha}}$		$\lambda_{2\alpha}$ $[\equiv \tilde{W}^\pm, \tilde{W}^0]$	$W^\pm, W^0$	$(\mathbf{1}, \mathbf{3}, 0)$	1
B	$\mathbf{W_{1\alpha}}$		$\lambda_{1\alpha}$ $[\equiv \tilde{B}]$	B	$(\mathbf{1}, \mathbf{1}, 0)$	1
DG-octet	$\mathbf{O}$	O	χ_g $[\equiv \tilde{g}']$		$(\mathbf{8}, \mathbf{1}, 0)$	0
DG-triplet	$\mathbf{T}$	$\{T^0, T^\pm\}$	$\{\chi^0_T, \chi^\pm_T\}$ $[\equiv \{\tilde{W}'^\pm, \tilde{W}'^0\}]$		$(\mathbf{1}, \mathbf{3}, 0)$	0
DG-singlet	$\mathbf{S}$	S	χ_S $[\equiv \tilde{B}']$		$(\mathbf{1}, \mathbf{1}, 0)$	0
Higgs-like	$\mathbf{R_u}$	R_u	$\tilde{R}_u$		$(\mathbf{1}, \mathbf{2}, -1/2)$	1
leptons	$\mathbf{R_d}$	R_d	$\tilde{R}_d$		$(\mathbf{1}, \mathbf{2}, 1/2)$	1
Fake	$\hat{\mathbf{E}}(\times 2)$	$\hat{E}$	$\hat{\tilde{E}}$		$(\mathbf{1}, \mathbf{1}, 1)$	0
electrons	$\hat{\mathbf{E}}'(\times 2)$	$\hat{E}'$	$\hat{\tilde{E}}'$		$(\mathbf{1}, \mathbf{1}, -1)$	2

2.1.1. Field content

The MDGSSM field content can be seen as the minimal set providing the MSSM gauginos a Dirac mass while preserving two-loop unification and perturbativity of gauge couplings. We summarised it in Table 1. In addition to the chiral multiplets transforming under the adjoint representations of the gauge groups, it includes new fields charged under the lepton number global symmetry. They consist of extra Higgs-like doublets[3] $\mathbf{R}_u, \mathbf{R}_d$ as well as two pairs of vector-like right-handed electron superfields $\mathbf{E}'_{1,2}$ in $(\mathbf{1}, \mathbf{1})_1$ and $\tilde{\mathbf{E}}'_{1,2}$ in $(\mathbf{1}, \mathbf{1})_{-1}$. Such states are compatible with an $(SU(3))^3$ Grand Unification gauge group. This is the minimal set which enables a "natural" unification (unification without mass thresholds tuning) similar to the MSSM.

The adjoint chiral multiplets contain new complex adjoint scalars, S, T and O:

$$S = \frac{S_R + i S_I}{\sqrt{2}}$$

$$T = \frac{1}{2\sqrt{2}} \begin{pmatrix} T_R + i T_I & \sqrt{2}(T_{+R} + i T_{+I}) \\ \sqrt{2}(T_{-R} + i T_{-I}) & -(T_R + i T_I) \end{pmatrix}$$

[3] The hypercharges are opposite with respect to the Higgs doublet in the MSSM to match the MRSSM notation for the same fields.

$$O^{(a)} = \frac{O_R^{(a)} + i\, O_I^{(a)}}{\sqrt{2}} \tag{2.1}$$

where the S_R, $O_R^{(a)}$, T_R, T_{-R}, T_{+R} and the S_I, $O_I^{(a)}$, T_I, T_{-I}, T_{+I} are real scalars and pseudo-scalars, respectively.

2.1.2. Lagrangian

The superpotential for these fields can be written as

$$W = W_{Yukawa} + W_{DG} + W_{RV} \tag{2.2}$$

where W_{Yukawa} contains the usual MSSM Yukawas part

$$W_{Yukawa} = Y_u^{ij} \mathbf{U^c}_i \mathbf{Q}_j \mathbf{H}_u - Y_d^{ij} \mathbf{D^c}_i \mathbf{Q}_j \mathbf{H}_d - Y_e^{ij} \mathbf{E^c}_i \mathbf{L}_j \mathbf{H_d} \tag{2.3}$$

W_{DG} contains the R-symmetric (according to the choice of R-charges in Table 1) contributions of the non-MSSM fields[4]

$$\begin{aligned} W_{DG} = {} & (\mu + \lambda_S \mathbf{S}) \mathbf{H_d} \mathbf{H_u} + \sqrt{2} \lambda_T \mathbf{H_d} \mathbf{T} \mathbf{H_u} \\ & (\mu_R + \lambda_{SR} \mathbf{S}) \mathbf{R_u} \mathbf{R_d} + 2 \lambda_{TR} \mathbf{R_u} \mathbf{T} \mathbf{R_d} \\ & + (\mu_{\hat{E}\, ij} + \lambda_{S\hat{E}^c\, ij} \mathbf{S}) \hat{\mathbf{E}}_i \hat{\mathbf{E}}'_j + \lambda_{SEij} \mathbf{S} \mathbf{E^c}_i \hat{\mathbf{E}}'_j \\ & + \lambda_{SLRi} \mathbf{S} \mathbf{L}_i \mathbf{R}_d + 2 \lambda_{TLRi} \mathbf{L}_i \mathbf{T} \mathbf{R_d} - Y_{\hat{E}i} \mathbf{R_u} \mathbf{H_d} \hat{\mathbf{E}}_i \\ & - Y_{LFV}^{ij} \mathbf{L_i} \cdot \mathbf{H_d} \hat{\mathbf{E}}_j - Y_{EFV}^{j} \mathbf{R_u} \mathbf{H_d} \mathbf{E^c}_j \ , \end{aligned} \tag{2.4}$$

while W_{RV} gathers the R-symmetry violating terms

$$\begin{aligned} W_{RV} = {} & L\mathbf{S} + \frac{\hat{M}_1}{2} \mathbf{S}^2 + \frac{\kappa}{3} \mathbf{S}^3 + \hat{M}_2 \mathrm{tr}(\mathbf{TT}) + \hat{M}_3 \mathrm{tr}(\mathbf{OO}) \\ & + \lambda_{ST} \mathbf{S} \mathrm{tr}(\mathbf{TT}) + \lambda_{SO} \mathbf{S} \mathrm{tr}(\mathbf{OO}) + \frac{\kappa_O}{3} \mathrm{tr}(\mathbf{OOO}) - Y_{\hat{E}'i} \mathbf{R_d} \mathbf{H_u} \hat{\mathbf{E}}'_i \\ \underset{\text{R-symmetry}}{\longrightarrow} {} & 0 \end{aligned} \tag{2.5}$$

In this work we shall, as in [12], consider scenarios where R-symmetry is preserved by the superpotential (and thus these terms vanish). However we shall also consider the possibility that they do not vanish – so the superpotential violates R, in particular λ_{SO} will play an important role in the following.

For simplicity and to avoid lepton-flavour-violation constraints, we shall only the terms of the first three lines of (2.4) to appear with sizable couplings; the contributions of the last two must be small enough to be negligible for the purpose of this work, so we shall set them to zero throughout.

For the soft SUSY-breaking terms, from the MSSM we retain only the bilinear terms – i.e. conventional mass-squared terms and the B_μ term. All the scalar trilinear and Majorana gaugino mass terms violate R-symmetry; while for B_μ we suppose that, since R-symmetry is a chiral symmetry, we are breaking R-symmetry in the Higgs sector – and in fact it is only in combination with the superpotential terms $\mu, \lambda_S, \lambda_T$ that the R-symmetry is violated. Hence in principle we can have an entirely R-preserving supersymmetry-breaking sector.

[4] Note that our coupling λ_T is normalised differently to [12,22,85], to match the normalisation used in SARAH.

The soft SUSY breaking terms beyond those of the MSSM consist of[5]:

- Dirac gaugino masses:

$$W_{\text{supersoft}} = \int d^2\theta\sqrt{2}\theta^\alpha \Big[m_{D1}\mathbf{S}W_{Y\,\alpha} + 2m_{D2}\text{tr}(\mathbf{T}W_{2\,\alpha}) + 2m_{D3}\text{tr}(\mathbf{O}W_{3\,\alpha}) \Big]. \tag{2.6}$$

- Soft terms associated with the adjoint scalars

$$\begin{aligned} -\Delta\mathcal{L}^{\text{scalar soft}}_{\text{adjoints}} &= m_S^2|S|^2 + \frac{1}{2}B_S(S^2 + h.c.) + 2m_T^2\text{tr}(T^\dagger T) + (B_T\text{tr}(TT) + h.c.) \\ &\quad + 2m_O^2\text{tr}(O^\dagger O) + (B_O\text{tr}(OO) + h.c.) \\ &\quad + \Big[T_S S H_u\cdot H_d + 2T_T H_d\cdot T H_u + \frac{1}{3}\kappa A_\kappa S^3 + t_S S + h.c.\Big] \\ &\quad + \Big[T_{SO}S\text{tr}(O^2) + T_{ST}S\text{tr}(T^2) + \frac{1}{3}T_O\text{tr}(O^3) + h.c.\Big] \end{aligned} \tag{2.7}$$

  The terms on the last line have generally been neglected, but will play an important role in this work.

- Soft terms involving the new vector-like leptons:

$$\begin{aligned} -\Delta\mathcal{L}^{\text{scalar soft}}_{\text{vector-like}} &= m^2_{R_u}|R_u|^2 + m^2_{R_d}|R_d|^2 + [B_R R_d R_u + h.c.] \\ &\quad + \hat{E}_i(m^2_{\hat{E}})^i_{\ j}\hat{E}^j + \hat{E}'^i(m^2_{\hat{E}'})^j_{\ i}\hat{E}'_j + [B^{ij}_{\hat{E}}\hat{E}_i\hat{E}'_j + h.c.] \\ &\quad + [T^{ij}_{SE}S\hat{E}_i\hat{E}'_j + T_{SR}SR_dR_u + h.c.]\,. \end{aligned} \tag{2.8}$$

Let us highlight that in an R-symmetry conserving model, one cannot simultaneously have the trilinears T_{SE} (respectively T_{SR}) from (2.8) and the superpotential couplings λ_{SE} (respectively λ_{SR}) from (2.4) as each term requires a different R-charge for the fields $\hat{E}$ and $\hat{E}'$ (respectively R_u and R_d) to be R-invariant.

2.1.3. Scalar mass matrix

We use the notation

$$\begin{aligned} \tilde{m}_S^2 &= \tilde{m}_{SR}^2 + \lambda_S^2\frac{v^2}{2} \\ \tilde{m}_T^2 &= \tilde{m}_{TR}^2 + \lambda_T^2\frac{v^2}{2}\,, \end{aligned} \tag{2.9}$$

where the effective masses for the real parts of S and T read:

$$\tilde{m}_{SR}^2 = m_S^2 + 4m_{1D}^2 + B_S, \qquad \tilde{m}_{TR}^2 = m_T^2 + 4m_{2D}^2 + B_T\,. \tag{2.10}$$

Then, at tree level the scalar mass matrix in the basis $\{h, H, S_R, T_R^0\}$ is [23]:

$$\begin{pmatrix} M_Z^2 + \Delta_h s_{2\beta}^2 & \Delta_h s_{2\beta}c_{2\beta} & \Delta_{hS} & \Delta_{hT} \\ \Delta_h s_{2\beta}c_{2\beta} & M_A^2 - \Delta_h s_{2\beta}^2 & \Delta_{HS} & \Delta_{HT} \\ \Delta_{hS} & \Delta_{HS} & \tilde{m}_S^2 & \lambda_S\lambda_T\frac{v^2}{2} \\ \Delta_{hT} & \Delta_{HT} & \lambda_S\lambda_T\frac{v^2}{2} & \tilde{m}_T^2 \end{pmatrix} \tag{2.11}$$

[5] We suppress gauge indices while retaining generation indices and denote the complex conjugation of fields by upper versus lower indices.

where we have defined:

$$\Delta_h = \frac{v^2}{2}(\lambda_S^2 + \lambda_T^2) - M_Z^2 \tag{2.12}$$

which vanishes when λ_S and λ_T take their $N = 2$ values,

$$\Delta_{hS} = -2\frac{v_S}{v}\tilde{m}_{SR}^2, \qquad \Delta_{hT} = -2\frac{v_T}{v}\tilde{m}_{TR}^2 \tag{2.13}$$

and

$$\Delta_{HS} = g' m_{1D} v s_{2\beta}, \qquad \Delta_{HT} = -g m_{2D} v s_{2\beta}\,. \tag{2.14}$$

This matrix is diagonalised by the mixing matrix S_{ij}. Of particular interest will be S_{11} which measures if the lightest scalar eigenstate is Standard Model Higgs like, and S_{13} which measures the proportion of the scalar singlet S_R in this lightest eigenstate.

3. Generating trilinear and quartic couplings

Previous studies of Dirac gaugino models have generally neglected the phenomenology of adjoint self-coupling terms, with an exception being a superpotential term $\frac{\kappa}{3}S^3$ used in [22] to generate μ/B_μ as in the NMSSM, and a recent brief discussion in [61]. In the case of superpotential terms such as λ_{SO} these can be neglected when considering an R-symmetric visible sector; however, trilinear soft couplings such as T_{SO}, T_O (see (2.7)) are always allowed. It is therefore interesting to consider what values we expect from models of supersymmetry-breaking mediation.

Starting with a spurion analysis where supersymmetry is broken by either a D-term D or F-term F, then if the mediating dynamics is at a scale M the terms in our effective Lagrangian should be given by powers of $\frac{D}{M}, \frac{F}{M}, \frac{D}{M^2}, \frac{F}{M^2}$ with appropriate factors of couplings and $\kappa_l \equiv 1/16\pi^2$. Furthermore, quartic and higher-order couplings – which are "hard" SUSY-breaking parameters – are always generated, but do not lead to quadratic divergences because they appear suppressed by powers of the scale M which is the cutoff of our effective theory. Important in this work are the quartics such as $\mathcal{L} \supset \frac{\lambda_{4S}}{24}S^4$ which must have size $\lambda_{4S} \sim \kappa_l^p \left(\frac{D}{M^2}\right)^q$ for some integer p, q (or similarly for F-terms with *even* q); taking $p = 1$, $q = 1$ for a D-term we naively have a quadratic divergence in the scalar mass proportional to λ_{4S} but this yields $\Delta m_S^2 \sim \kappa_l \lambda_{4S} M^2 \sim \kappa_l^2 D \ll M^2$, while for $q = 2$ we have $\kappa_l^2 \frac{D^2}{M^2}$. In fact, this tells us that the case $q = 1$ is special because it implies a much larger correction at one loop than the direct mass, and could therefore destabilise the calculation. We shall return to this below.

As a first observation, if the mediation is by gravity, then M should be identified with the Planck scale (unless there is significant sequestering) and we should only consider the leading order terms. We would therefore require the quantum gravity theory to give us the terms T_{SO}, T_O at leading order D/M, F/M and the quartics must, by the above reasoning, be negligible.

On the other hand, in the case of low-scale supersymmetry breaking – where it was argued in [86] that this requires Dirac gauginos – $\sqrt{F} \sim \sqrt{D} \sim M \sim$ TeV, and we generate all terms at a similar order, which would include T_{SO}, T_O. However, the phenomenology is significantly changed by the presence of higher-dimensional operators and the goldstino couplings [55] and, since it is difficult to reconcile with perturbative unification, we shall not discuss this further here.

Finally, for gauge mediation M could be as small as $\sqrt{F}$ or $\sqrt{D}$ but there is no a priori upper limit on M until we choose a particular quantum gravity embedding. The Dirac gaugino masses are expected to be generated at one loop and be of order $\kappa_l \frac{D}{M}$ or $\kappa_l \frac{F^2}{M^3}$. For F-term breaking the standard gauge-mediation soft mass-squareds for the squarks/sleptons are of order $\kappa_l^2 \frac{F^2}{M^2}$, while in D-term breaking they may be suppressed. Therefore if we imagine that $\kappa_l \frac{D}{M} \sim$ TeV, then for terms $\kappa_l \frac{D^2}{M^3}$ to be significant we would need $D \sim M^2$ and furthermore $M \sim 100$ TeV.

3.1. Adjoint couplings in gauge mediation

One of the most interesting issues in the construction of gauge mediation models with Dirac gaugino masses has been that of the adjoint scalar masses: in the simplest realisation, only a B-type mass-squared $\mathcal{L} \supset -\frac{1}{2} B_\Sigma \Sigma^2$ is generated at leading order in D/M^2, and not a conventional mass-squared $\mathcal{L} \supset -m_\Sigma^2 |\Sigma|^2$. This happens for one pair of vector-like messengers $Q, \tilde{Q}$ having charges under a hidden $U(1)$ of $+1, -1$, where the $U(1)$ obtains a D-term. This was noticed from the earliest models [30,87] with the original proposed solution being to add a supersymmetric mass for the adjoint – which would also violate the R-symmetry and generate Majorana masses for the gauginos, with a see-saw effect. However, an alternative solution was found to be to introduce additional messenger states with non-diagonal couplings to either the adjoints (in the D-term case) [33,36] or an F-term spurion [31,33,36]; in the D-term case this requires the couplings to violate the $U(1)$-charges. In [36] examples were given where the ratio of B-type to conventional masses is arbitrary. The general ansatz was to couple the adjoint to messenger fields $Q_i, \tilde{Q}_j$ and to possible F-term spurions X via superpotential couplings

$$W \supset M Q_i \tilde{Q}_i + \lambda_{i\tilde{j}} Q_i \Sigma \tilde{Q}_j + \mu_{i\tilde{j}} X Q_i \tilde{Q}_j \tag{3.1}$$

and D-terms via charges $e_i, \tilde{e}_i$ which we can write as a matrix $e_{i\bar{j}}(Q_i Q_j^* - \tilde{Q}_i \tilde{Q}_j^*)$.

More recently, the issue has been re-examined. One suggested approach, dubbed "Goldstone gauginos," is to promote the adjoints to be the Goldstone bosons of a broken symmetry [59,60]; however, this solution would lead effectively to no higher-order interactions for our adjoint scalars and we do not consider it here. More in the spirit of the earlier works, the issue was rephrased in the language of effective operators in [38,52,61], where it was claimed that the explanation for the absence of conventional mass-squared terms for the adjoints at leading order is that the operator responsible for the generation of a leading-order mass-squared term should be

$$\mathcal{L} \supset \int d^4\theta \frac{1}{M^2} [\psi^\dagger e^{qV} \psi + \tilde{\psi}^\dagger e^{-qV} \tilde{\psi}] \Sigma^\dagger \Sigma, \tag{3.2}$$

where $\psi, \tilde{\psi}$ are a pair of fields charged under the hidden $U(1)$ with charges $\pm q$ which obtain vevs (and thus generate a contribution to the hidden D-term). The above operator is generated by including terms in the superpotential that mix the messengers $Q, \tilde{Q}$ with other pairs of fields $N, \tilde{N}$ which are neutral (or at least have different charges) under the hidden $U(1)$, so that the vevs of $\psi, \tilde{\psi}$ generate messenger mixing terms. This is clearly nearly equivalent to the above ansatz, and can be written in the form

$$W \supset M_{ij} Q_i \tilde{Q}_j + \lambda_i Q_i \Sigma \tilde{Q}_i \tag{3.3}$$

where we now write the mass terms as violating the $U(1)$ charges instead.

If we start with the case of no couplings/mass mixing terms that violate the $U(1)$ D-term charges, we shall first give a simple proof that the conventional mass term $|\Sigma|^2$ vanishes at leading order for any number of messengers, and then look at higher-order terms. Considering first the visible gauge group to be $U(1)$, we have the effective potential contribution from the messenger scalars (since the fermion potential is independent of D):

$$V = \int \frac{d^d q}{(2\pi)^d} \mathrm{tr}\log(q^2 + \mathcal{M}_Q^2 + De) + \mathrm{tr}\log(q^2 + \mathcal{M}_{\tilde{Q}}^2 - De)$$
$$\equiv V_+ + V_-. \tag{3.4}$$

Here $\mathcal{M}_Q^2 = (M + \lambda\Sigma)(M^\dagger + \lambda^\dagger\overline{\Sigma})$, $\mathcal{M}_{\tilde{Q}}^2 = (M^\dagger + \lambda^\dagger\overline{\Sigma})(M + \lambda\Sigma)$ are the supersymmetric mass-squared matrices. Now, if we take the couplings to preserve the $U(1)$ charges then we can write

$$V_+ = De \int \frac{d^d q}{(2\pi)^d} \mathrm{tr}\left(\frac{1}{q^2 + \mathcal{M}_Q^2}\right) - \frac{1}{2} D^2 e^2 \int \frac{d^d q}{(2\pi)^d} \mathrm{tr}\left(\frac{1}{q^2 + \mathcal{M}_Q^2}\right)^2 + \mathcal{O}(D^3)$$
$$\to 16\pi^2 V = D^2 e^2 \mathrm{tr}\left(\log \mathcal{M}_Q^2/\mu^2\right) + \mathcal{O}(D^4) \tag{3.5}$$

since the eigenvalues of $\mathcal{M}_Q^2$ and $\mathcal{M}_{\tilde{Q}}^2$ are equal. Next, by taking the derivative with respect to Σ we find only a holomorphic function of Σ:

$$16\pi^2 \frac{\partial V}{\partial \Sigma} = D^2 e^2 \mathrm{tr}\left([M + \lambda\Sigma]^{-1}\lambda\right) + \mathcal{O}(D^4)$$
$$\to V = \frac{D^2 e^2}{16\pi^2}\left[\mathrm{tr}\left(\log M M^\dagger/\mu^2\right) + \tilde{V}(\Sigma) + \overline{\tilde{V}}(\overline{\Sigma})\right] + \mathcal{O}(D^4). \tag{3.6}$$

As an example, consider the simple model of a single messenger where the matrices become numbers; then we have

$$\tilde{V}(\Sigma) = -\sum_{n=1}^{\infty} \frac{1}{n}\left(\frac{-\lambda\Sigma}{M}\right)^n. \tag{3.7}$$

This potential manifestly has trilinear and quartic couplings, although at order $\frac{D^2}{M^3}$, $\frac{D^2}{M^4}$ respectively. Indeed, if we continue with the ansatz (3.1) then it is easy to see that there are no terms of linear order in D, because $\mathcal{M}_Q^2 = (M + \lambda\Sigma)(M + \lambda^\dagger\Sigma^\dagger) = \mathcal{M}_{\tilde{Q}}^2$ and

$$V = D \int \frac{d^d q}{(2\pi)^d} \mathrm{tr}\left\{\left([q^2 + \mathcal{M}_Q^2]^{-1} - [q^2 + \mathcal{M}_{\tilde{Q}}^2]^{-1}\right)e\right\} + \mathcal{O}(D^2). \tag{3.8}$$

Hence to have large cubic interactions we should start from ansatz (3.3). In this way, in order to have an interesting phenomenology we require either $D \sim M^2$ with both at a low scale, or we require (as proposed in [52]) that

$$B_\Sigma < m_\Sigma^2 \sim aD + b\frac{D^2}{M^2} \tag{3.9}$$

with some cancellation between the two terms so that we can have $m_\Sigma \sim T_{SO}$. Note that once we take this ansatz with non-zero mixing between the messengers and $[M, e] \neq 0$ we typically

generate trilinear terms in the potential – but also tadpoles. The issue of tadpoles is then easily circumvented by embedding the coupling of the singlet adjoint S to the $SU(3)$ and $SU(2)$ adjoints into the generator $T^Y = \frac{1}{\sqrt{60}}\text{diag}(2,2,2,-3,-3)$. This then also means that the couplings of the singlet adjoint S are related to those of T and O; for example, for T_{SO}, if we have calculated the coupling for $U(1)$ messengers as being $\mathcal{L} \supset \frac{1}{6} T_\Sigma \Sigma^3$, then we have

$$\begin{aligned} T_{SO}\delta^{ab} &= T_\Sigma \text{tr}(T^Y T_3^a T_3^b) \\ &= \frac{1}{\sqrt{15}} T_\Sigma \delta^{ab} \end{aligned} \tag{3.10}$$

where T_3^a, T_3^b are $SU(3)$ generators. However, exploring sets of messengers which give these desired properties with sufficiently large trilinear couplings and exploring the vacuum stability of the total system would be very interesting, but is beyond the scope of this work.

4. Constraining the MDGSSM from the diphoton excess

We analyse in this section various theoretical and experimental constraints lying on the general model presented above. We start by considering the basics of production and decay of the scalar singlet and then study the most relevant collider constraints on our model. We finally investigate the requirements we need to impose in order to remain perturbative up to the GUT scale and avoid the appearance of Charge or Colour Breaking Vacuua.

4.1. Production and decay in the MDGSSM

In the narrow width approximation in which the mediating Φ singlet is automatically on-shell, we can approximate the cross section of the complete process $pp \to \Phi \to \gamma\gamma$ as follows:

$$\sigma(pp \to \Phi \to \gamma\gamma) = \frac{2J+1}{s m_\Phi \Gamma}\left[C_{gg}\Gamma(\Phi \to gg) + \sum_q C_{q\bar{q}}\Gamma(\Phi \to q\bar{q})\right]\Gamma(\Phi \to \gamma\gamma)\,. \tag{4.1}$$

Assuming a spin-zero particle of mass m_Φ produced resonantly via gluon fusion, we arrive at

$$\begin{aligned} \sigma(pp \to \Phi \to \gamma\gamma)_{13\text{ TeV}} &\approx K_{13} \times 4.9 \times 10^6 \text{ fb} \frac{\Gamma_{gg}}{\Gamma}\frac{\Gamma_{\gamma\gamma}}{\Gamma}\frac{\Gamma}{m_\Phi} \\ \sigma(pp \to \Phi \to \gamma\gamma)_{8\text{ TeV}} &\approx K_8 \times 1.1 \times 10^6 \text{ fb} \frac{\Gamma_{gg}}{\Gamma}\frac{\Gamma_{\gamma\gamma}}{\Gamma}\frac{\Gamma}{m_\Phi}\,, \end{aligned} \tag{4.2}$$

taking $C_{gg}^{8\text{ TeV}} = 174$ and $C_{gg}^{13\text{ TeV}} = 2137$ as values arising from the parton distribution functions [81], respectively. An important aspect of our calculation is that for a more realistic estimation, we have taken into account the K-factors $K_{8,13}$ for the full N^{m}LO production of $H+$jet compared to the tree-level process. We have estimated $K_8 \simeq 1.9$ from the comparison of the leading-order effective vertex from `MadGraph` and the Higgs Cross-section working group value for a Standard-Model-like Higgs of 750 GeV at 8 TeV. We will take conservatively the same value for K_{13}.

Let us first consider the coupling to two gluons. Considering our real scalar candidate S_R, the process $S_R \to gg$ is a priori generated by loops of squarks, scalar octet and gluinos. The width is given by

$$\Gamma(S_R \to gg) = \frac{\alpha_3^2 m_{S_R}}{8\pi^3}\left|\sum_f C_f \frac{g_{Sff}}{\sqrt{\tau_f}} A_{1/2}^S(\tau_f) + \sum_\phi C_\phi \frac{g_{S\phi\phi}}{2\sqrt{\tau_\phi} m_\phi} A_0^S(\tau_\phi)\right|^2 \tag{4.3}$$

$$\to \frac{\Gamma(S_R \to gg)}{m_{S_R}} \simeq 3\cdot 10^{-5}\left|\sum \frac{g_{Sff}}{\sqrt{\tau_f}} A_{1/2}^S(\tau_f) + \frac{g_{S\phi\phi}}{2\sqrt{\tau_\phi} m_\phi} A_0^S(\tau_\phi)\right|^2 ,$$

where we used $\alpha_s(m_{S_R}) \sim 0.09$, we have defined $\tau_i \equiv 4\frac{m_i^2}{m_{S_R}^2}$, the sums runs over all scalars and fermions, and

$$f(\tau) \equiv \begin{cases} (\sin^{-1}(1/\sqrt{\tau}))^2 & \tau \geq 1 \\ -\frac{1}{4}\left[\log\frac{1+\sqrt{1-\tau}}{1-\sqrt{1-\tau}} - i\pi\right]^2 & \tau < 1 \end{cases}$$

$$A_0^S = \tau(\tau f(\tau) - 1)$$

$$A_{1/2}^S = 2\tau\big(1 + (1-\tau) f(\tau))\big) .$$

C_f and C_ϕ indicate the corresponding colour factors, g_{Sff} and $g_{S\phi\phi}$ are the couplings with the singlet of the fermions and scalars participating in the triangular loops. The loop functions A_0^S and $A_{1/2}^S$ have a maximum at the resonant mass $m_{S_R}/2 \sim 375$ GeV. We will therefore generically require masses close to this scale in order to enhance the cross-section. The main contributions to the loop will be:

- D-term-induced couplings between the squarks and the singlet, generated by the Dirac masses operator of Eq. (2.6). Theses couplings are proportional to the hypercharge of the squarks and the Dirac mass m_{1D}. They are sizeable only for large Dirac mass m_{1D}.
- Soft terms trilinears couplings from (2.8) between the adjoint scalar octet and the singlet. They give a sizeable contribution but unfortunately are strongly constrained from vacuum stability bounds.

A priori, one could have expected a contribution from the Dirac gluinos. However, we observed that pure Dirac gluinos do not contribute at all to the amplitude. This remark is of crucial importance for the pseudo-scalar S_I which can only couple to gluons through fermions loops as we assume CP-conserving interactions. If no Majorana masses for the original gluinos are introduced, the pseudo-scalar is practically not produced. However, if we allow for the presence of an additional Majorana mass term, the pseudo-scalar S_I can then participate in the $\Phi \to \gamma\gamma$ cross-section, potentially leading to a "double-peak" scenario, as we will see later.

We now turn to the amplitude to diphotons. This is given for our scalar by

$$\Gamma(S_R \to \gamma\gamma) = \frac{\alpha^2 m_{S_R}}{64\pi^3}\left|\sum_f \frac{g_{Sff}}{\sqrt{\tau_f}} Q_f^2 A_{1/2}^S(\tau_f) + \sum_\phi \frac{g_{S\phi\phi}}{2\sqrt{\tau_\phi} m_\phi} Q_\phi^2 A_0^S(\tau_\phi)\right|^2 \tag{4.4}$$

$$\to \frac{\Gamma(\Phi \to \gamma\gamma)}{m_{S_R}} \simeq 2.7\cdot 10^{-8}\left|\sum \frac{g_{Sff}}{\sqrt{\tau_f}} A_{1/2}^S(\tau_f) + \frac{g_{S\phi\phi}}{2\sqrt{\tau_\phi} m_\phi} A_0^S(\tau_\phi)\right|^2 ,$$

where Q_f and Q_ϕ are the corresponding electric charges of the fermions and scalars running in the loops. In order to have an idea of the enhancement we need from the square term, let us find

the smallest value of $\Gamma_{\gamma\gamma}$ leading to a $\sigma(S_R \to \gamma\gamma) \gtrsim 2$ fb. In the limit in which Γ_{gg} dominates the decay width, we can use Eq. (4.2) to get

$$\frac{\Gamma_{\gamma\gamma}}{m_{S_R}} \gtrsim 2.1 \times 10^{-7}, \tag{4.5}$$

which is an order of magnitude larger than the numerical factor in (4.4). The key issue will therefore be to populate the sums in the square terms of (4.4) since the amplitude will very roughly scale as N^2, with N the number of particles participating in the loop. The main contributions will come from

- D-term-induced couplings between the sleptons and the singlet, they are again proportional to the hypercharge of the sleptons and to the Dirac mass m_{1D}. They are therefore sizeable only for large Dirac mass.
- Superpotential-induced couplings between the fake leptons and the singlet from the terms of (2.4) in section 2. They are the main contributions in our model.[6]
- Soft terms trilinears couplings from (2.8) between the fake sleptons and the singlet. They are again strongly constrained from vacuum stability bounds.

An important remark here is that the two last contributions are mutually incompatible in presence of a preserved R-symmetry as we already stressed in Section 2.1.2.

4.2. *Constraints from Higgs mass mixing and 8 TeV data*

A crucial property of the singlet S is that it will in general mix with the Higgs eigenstates. This is in our case an undesirable feature since it will lead to tree-level decays of S into tops, W, Z or Higgs which could easily overcome the one-loop decay into photons.

4.2.1. *Analytical estimate*

Building on the notations introduced in the previous sections, we can use the minimisation condition of v_S on the off-diagonal element Δ_{hS} of the scalar mass matrix given in (2.13) to find (see [88])

$$\begin{aligned}\Delta_{hS} =&\ v[v_S\lambda_S^2 - g' m_{1D} c_{2\beta} + \sqrt{2}\lambda_S\mu + \lambda_S\lambda_T v_T] \\ =&\ v[\sqrt{2}\lambda_S\tilde{\mu} - g' m_{1D} c_{2\beta}]\,,\end{aligned} \tag{4.6}$$

where we used the effective mass parameter

$$\tilde{\mu} = \mu + \frac{1}{\sqrt{2}}(\lambda_S v_S + \lambda_T v_T)\,. \tag{4.7}$$

From this basic analytical calculation, we see that we can minimise the tree-level mixing by choosing:

$$\lambda_S \sim \frac{g_Y m_{1D} c_{2\beta}}{\sqrt{2}\tilde{\mu}}\,. \tag{4.8}$$

In general, this relation will be modified at one-loop, but the property that one value of λ_S is favoured will remain and is easily observable in our coming Figures.

[6] Notice that since the coupling λ_S is usually small in most of the scenarios we will consider, the Higgsinos contribution will also be small.

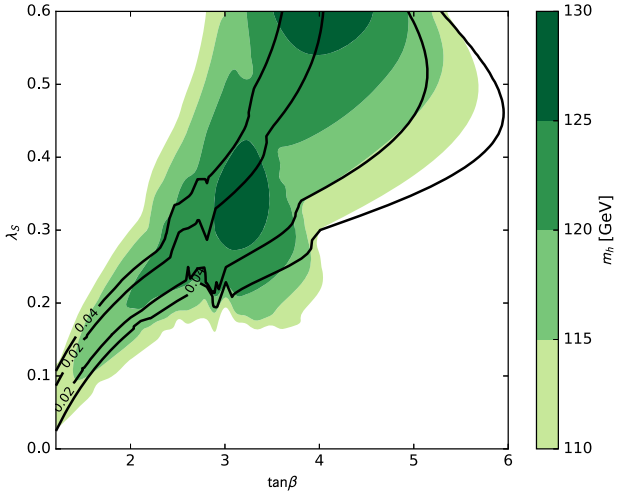

Fig. 1. Higgs mass and mixing between h and S_R as a function of λ_S and $\tan\beta$. The thin black lines represent the 2% and 4% mixing contour lines. The anomalies around $\tan\beta \sim 2.5$ corresponds to the region where the two-loop effective potential used to determined the Higgs mass suffers from the so-called "Goldstone boson catastrophy" (see [75] for more details).

4.2.2. Experimental bounds and naturalness

Such a mixing with the Standard Model Higgs will modify the Higgs sector observables. From [89] we find the latest constraint on the 125 GeV Higgs global signal strength μ_{average} to be

$$\mu_{\text{average}} = 1.09^{+0.11}_{-0.10} \,. \tag{4.9}$$

In our case this is modified by a factor of $|S_{11}|^2$, where S is the mixing matrices of the scalar sector; the above constraint gives us

$$1 - |S_{11}|^2 \leq 0.24 \leftrightarrow \sum_{k\neq 1} |S_{1k}|^2 = \sum_{k\neq 1} |S_{k1}|^2 \leq 0.24. \tag{4.10}$$

This condition is in fact satisfied quite easily, as can be seen from Fig. 1 where we show the contours for the Higgs mass and the mixing matrix element S_{31} as a function of $\tan\beta$ and λ_S. An important comment regarding this Figure is that a 125 GeV Higgs boson also favours small mixing.

More stringent constraints arise from the non-observation of any excess in the 8 TeV data for the ZZ, and hh, dijets and WW channels: $\sigma^{\text{LHC8}}_{hh} < 39$ fb [90], $\sigma^{\text{LHC8}}_{ZZ} < 12$ fb [91], $\sigma^{\text{LHC8}}_{Zh} < 19$ fb [92], $\sigma^{\text{LHC8}}_{W^+W^-} < 40$ fb [93,94]. Assuming dominant production of the singlet via gluon fusion, we can approximate a scaling factor of $\sigma^{13\text{ TeV}}/\sigma^{8\text{ TeV}} \approx 5$, which lead to the following bounds under consideration of $\sigma^{13\text{ TeV}} \cdot B_{\gamma\gamma} \approx 3.7 \pm 2$ fb:

$$\left.\begin{array}{rl} \Gamma(S_R \to hh) & \lesssim 53 \\ \Gamma(S_R \to ZZ) & \lesssim 16 \\ \Gamma(S_R \to Zh) & \lesssim 26 \\ \Gamma(S_R \to WW) & \lesssim 54 \end{array}\right\} \times \Gamma(S_R \to \gamma\gamma) \times \left(\frac{3.7\text{ fb}}{\sigma^{13\text{ TeV}} \cdot B_{\gamma\gamma}}\right) \tag{4.11}$$

which gives the most stringent constraints on the mixing between S and h. The di-Higgs channel is proportional to the tree-level mixing term without passing through the mixing, because the vertex is given by Δ_{hs}/v (plus smaller terms proportional to the mixing matrix elements S_{13}, S_{31}); we have

$$\begin{aligned}\frac{\Gamma(S_R \to hh)}{m_{S_R}} &\simeq \left(\frac{\Delta_{hs}}{v}\right)^2 \frac{1}{32\pi \tilde{m}^2_{SR}} \sqrt{1-\frac{4m_h^2}{\tilde{m}^2_{SR}}} \\ &\simeq 0.01 \times \left(\frac{\tilde{m}^2_{SR}}{v^2}\right)\left(\frac{\Delta_{hs}}{m^2_{SR}}\right)^2 \\ &\simeq 0.1 \times |S_{13}|^2, \end{aligned} \tag{4.12}$$

which gives a constraint of $S_{13} \lesssim 0.01$. On the other hand the constraints for Z and W decays come purely through the mixing matrix; defining $x \equiv \frac{m_V^2}{m^2_{S_R}}$ for a vector boson V we have a decay rate

$$\Gamma(S_R \to VV) = \frac{|c_{sVV}|^2}{128\pi m_V} x^{-3/2}(1-4x+12x^2)\sqrt{1-4x} \tag{4.13}$$

and

$$c_{hZZ} = \frac{g_Y^2+g_2^2}{2}v = \frac{2M_Z^2}{v}, \quad c_{hW^+W^-} = \frac{g_2^2 v}{2} \simeq \frac{2M_W^2}{v}, \quad c_{tW^+W^-} = 2g_2^2 v_T. \tag{4.14}$$

Neglecting v_T and mixing with the triplet as small effects, we can then write

$$\begin{aligned}\frac{\Gamma(S_R \to ZZ)}{m_{S_R}} &\simeq 0.09|S_{13}|^2 \\ \frac{\Gamma(S_R \to WW)}{m_{S_R}} &\simeq 0.17|S_{13}|^2. \end{aligned} \tag{4.15}$$

Translating these into constraints, we see that it is the Z decays which are most important.

Notice that the only loop decays included in this paper are $S_R \to \gamma\gamma$ and $S_R \to gg$ (as they do not have a tree-level contribution). A priori in the negligible mixing region, one should also consider the other diboson loop decays (in particular to $Z\gamma$). However, almost all of the new fields contributing to the loop decays will be $SU(2)$ singlets so that the decay to diphoton will be the dominant diboson decay channel. The only exceptions are the new doublets $\mathbf{R}_u$ and $\mathbf{R}_d$ which should mostly decay to WW, ZZ and $Z\gamma$. Due to the interference with the tree-level processes the loop contribution to these processes is not currently calculated in SARAH; their implementation is eagerly awaited in future work, but here we note that they will not have a significant impact on our results as described in [11].

Finally, the VEV of T gives a contribution to the W boson mass and the electroweak precision data give bounds on it. One must examine the induced correction $\Delta\rho$ to the Veltman ρ-parameter:

$$\rho \equiv \frac{M_W^2}{c^2_{\theta_W} M_Z^2} = 1 + \Delta\rho\ , \tag{4.16}$$

with $\Delta\rho$ given analytically at tree-level by ([88])

$$\Delta\rho \sim \frac{4v_T^2}{v^2}\ , \tag{4.17}$$

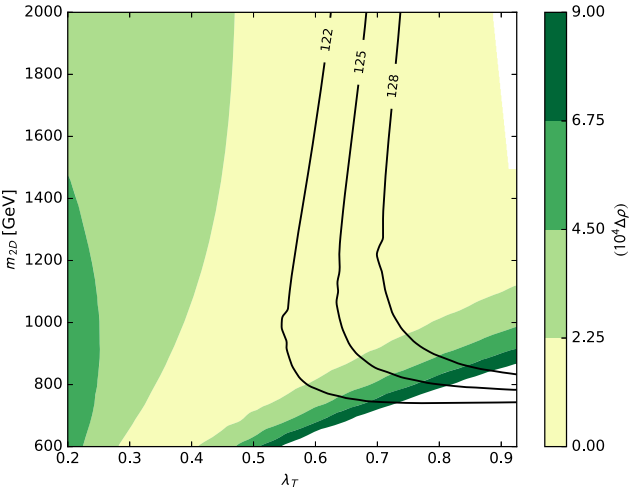

Fig. 2. One-loop $(10^4 \cdot \Delta\rho)$ in scenario $\mathbf{R_a}$ obtained from the benchmark point of Table 2 by varying λ_T and m_{2D}. We have taken $m_T = 450$ GeV. The black lines give the contours for $m_H = 122,\ 125$ and 128.

where v is the usual Standard Model Higgs VEV. In order to be below the experimental constraints, we need $\Delta\rho \lesssim (4.2 \pm 2.7) \times 10^{-4}$, ([88] – see also [24,54] –). At tree level, we have

$$v_T \simeq \frac{v^2}{2\tilde{m}_{TR}^2} \left[-g m_{2D} c_{2\beta} - \sqrt{2}\tilde{\mu}\lambda_T \right], \tag{4.18}$$

with $\tilde{m}_{TR}^2 = m_T^2 + 4m_{2D}^2 + B_T$, therefore, small $\Delta\rho$ require large triplet Dirac and soft masses. This requirement can often be at odd with naturalness which prefers smaller triplet masses. Indeed, radiative corrections induced by the adjoint triplet scalars to $m_{H_{u,d}}^2$ are [88]:

$$\delta m_{H_{u,d}}^2 \supset -\frac{1}{16\pi^2}(2\lambda_T^2 m_T^2) \log\left\{\frac{\Lambda}{\text{TeV}}\right\}, \tag{4.19}$$

with Λ the UV cut-off, $m_{H_{u,d}}^2, m_T^2$ the squared masses for Higgses and scalar triplet T, and λ_T the coupling defined in (2.4). For Λ at the Planck scale, requiring a fine-tuning $\Delta_T = \delta m_H^2/m_H^2$ better than 10% finally gives us

$$m_T \lesssim \frac{1}{\lambda_T} 450 \text{ GeV}. \tag{4.20}$$

In Fig. 2, we show the allowed region for λ_T and m_{2D} for $m_T = 450$ GeV. $\Delta\rho$ has been obtained at one-loop using the Spheno [72,73] code generated by SARAH (see Refs. [66–70]). We see that the Higgs mass prefer large values of λ_T but that the following three requirements are perfectly compatible: (1) a 125 GeV Higgs, (2) a natural mass for the triplet and (3) a parameter $\Delta\rho$ smaller than the current constraints.

4.3. Bounds on colour octets

In this work we shall be interested in the case when either the scalar or pseudoscalar colour octets are lighter than a TeV. Even though such light scalars should be copiously produced in

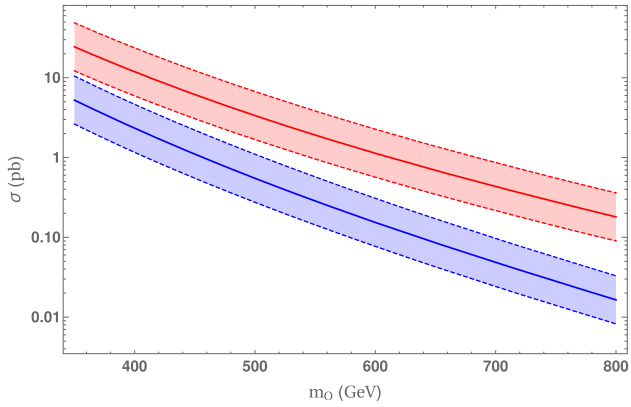

Fig. 3. Pair production cross-section of octets at tree-level, at 8 TeV (blue, lower curves) and 13 TeV (red, upper curves). The bands indicate a variation of a factor of 2 each way relative to the values obtained in `MadGraph`. (For interpretation of the references to colour in this figure legend, the reader is referred to the web version of this article.)

pairs at both 8 and 13 TeV, as shown in Fig. 3, their decays are loop suppressed and this inhibits single production.

Since current limits place all squarks above about 800 GeV, then, as first discussed in [32,95], the octets decay only to gluons and quarks – in particular almost entirely top quarks. This means that the possible signatures are four jets, dijet/ditop searches, and four tops. Up until relatively recently the constraints on them were rather weak, with dijets providing no constraint, and a mild constraint from ditops [96]. However, now the four top channel is particularly important: [97] placed a limit of 32 fb at 8 TeV, and [98] found 370 fb for Standard-Model-like kinematics, or 140 fb with and EFT pointlike interaction, at 13 TeV.

To interpret the implications of these searches for our model, we could in principle do a full recasting along the lines of [99]; however, for simplicity we shall consider instead the cross-section times branching ratio approach, taking the most conservative values of twice the tree-level cross-section (i.e. a K-factor of 2) and a limit at 13 TeV of 140 fb. To compute the branching ratio into four tops, we require the widths into gluons and tops; while expressions were given for these originally in [32,95], those papers used *complex* octets, which is not appropriate for our case where the necessarily large ($\gtrsim 2$ TeV) gluino mass causes a large splitting. Instead we require the expressions presented in [55], which we shall not reproduce here but to which we refer the reader.

The first important observation is that the pseudoscalar octet *does not couple* to gluons, and so pair production of pseudoscalar octets yields only four-top events, and by our above criteria excludes pseudoscalars below about 880 GeV *by the* 13 *TeV data.* These are therefore less interesting for our analysis.

On the other hand, the scalar octet couples to squarks via its D-term coupling, and so couples to gluons. Since it couples to *all* coloured squarks, this can potentially be large. However, to be very conservative, we show production times branching ratio of four-tops via scalar octets in Fig. 4 at 8 and 13 TeV with the limits shown using a K-factor of 2, as we vary the octet mass and for three different values of the Dirac gluino mass, where the first two generations of squarks are decoupled (i.e. heavy and degenerate). To produce these, we take left-handed stops and sbottoms of 1200 GeV, right-handed stops of 800 GeV, and decoupled right-handed sbottoms (at 4 TeV). We neglect all squark mixing (which is a good approximation in this model). Since the

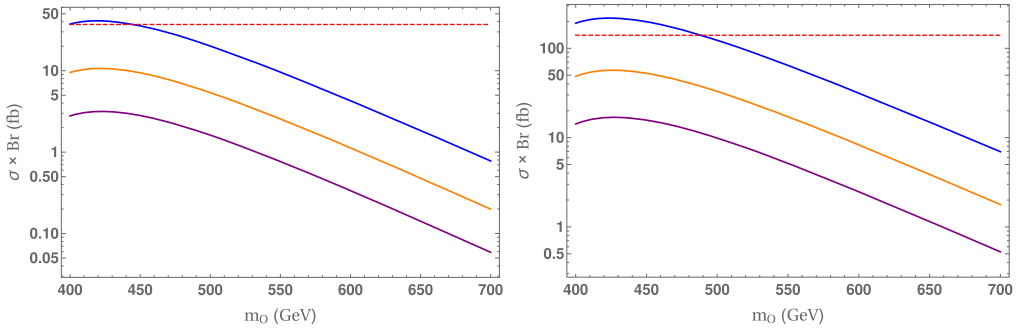

Fig. 4. Four-top production times branching ratio from scalar colour octets as a function of the octet mass, for gluino masses of 2.5 TeV (upper curve, blue), 3 TeV (middle curve, orange) and 3.5 TeV (lower curve, purple). The experimental limit is shown as the dashed red horizontal line. The left plot is computed for $\sqrt{s} = 8$ TeV, and right is for $\sqrt{s} = 13$ TeV. (For interpretation of the references to colour in this figure legend, the reader is referred to the web version of this article.)

couplings involve a cancellation between left- and right-handed squarks, this is very conservative: if we took heavier left-handed squarks, we would enhance the gluon rate relative to the top rate (because it has a contribution from sbottoms as well as stops) weakening the bounds.

We conclude that for 2.5 GeV gluinos, the octet scalars must be heavier than 500 GeV; but for 3 TeV gluinos there is no constraint.

4.4. *Perturbativity and Landau poles*

The field content of the MDGSSM, and more precisely the two pairs of vector-like electrons $\hat{E}$ and $\hat{E}'$ as well as the doublet R_u, R_d, have been chosen to have one-loop unification by completing the $\mathbf{8}_0 + \mathbf{3}_0 + \mathbf{1}_0$ set of adjoint multiplets into a complete GUT representation of $(SU(3))^3$ (see [12]). We have furthermore checked numerically that gauge couplings remain safely perturbative at two-loops up to the GUT scale, consistently with the results of [12].

Once the GUT scale is determined, we require perturbation theory to be valid up to the GUT scale. We choose as perturbativity requirement that all Yukawa couplings should remain smaller than $\sqrt{4\pi}$. As we will see now, this gives strong constraints on the Yukawa couplings. At one-loop, the beta functions for λ_{SE}, λ_{SR}, λ_{SO}, λ_S and λ_T form a coupled system given by:

$$\begin{aligned}
\beta_{\lambda_S} &= \frac{1}{16\pi^2}\lambda_S[4\lambda_S^2 + 3\lambda_T^2 + 2\lambda_{SR}^2 + 2\lambda_{SE}^2 + 4\lambda_{SO}^2 - \frac{3}{5}g_1^2 - 3g_2^2 + 3y_t^2 + \dots] \\
\beta_{\lambda_T} &= \frac{1}{16\pi^2}\lambda_T[2\lambda_S^2 + 4\lambda_T^2 - \frac{3}{5}g_1^2 - 7g_2^2 + 3y_t^2 \dots] \\
\beta_{\lambda_{SE}} &= \frac{1}{16\pi^2}\lambda_{SE}[2\lambda_S^2 + 4\lambda_{SE}^2 + 2\lambda_{SR}^2 + 4\lambda_{SO}^2 - \frac{12}{5}g_1^2 + \dots] \\
\beta_{\lambda_{SR}} &= \frac{1}{16\pi^2}\lambda_{SR}[2\lambda_S^2 + 2\lambda_{SE}^2 + 4\lambda_{SR}^2 + 4\lambda_{SO}^2 - \frac{3}{5}g_1^2 - 3g_2^2 + \dots] \\
\beta_{\lambda_{SO}} &= \frac{1}{16\pi^2}\lambda_{SO}[2\lambda_S^2 + 4\lambda_{SE}^2 + 2\lambda_{SR}^2 + 6\lambda_{SO}^2 - 12g_3^2 + \dots] ,
\end{aligned}$$

where the dots contain the contributions from the other couplings. Before studying this system numerically, we point out some peculiarities of these expressions:

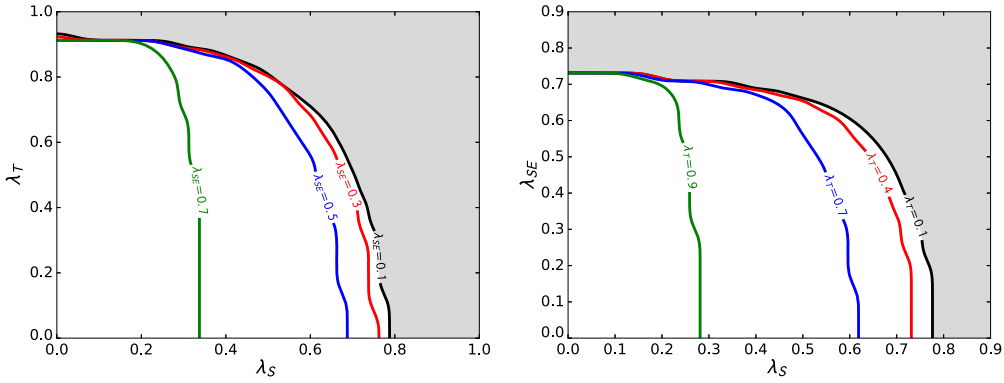

Fig. 5. Perturbativity bounds on our model, around the first benchmark point from Table 2, obtained from the requirement that no couplings overtake $\sqrt{4\pi}$ before the GUT scale. We consider $\lambda_{SR} = \lambda_{SE}$. Left plot: Bounds for (from left to right) $\lambda_{SE} = 0.7, 0.5, 0.3, 0.1$ in the λ_S/λ_T plane, all points above the curves are excluded. Right plot: Bounds for (from left to right) $\lambda_T = 0.9, 0.7, 0.4, 0.1$ in the λ_S/λ_{SE} plane, all points above the curves are excluded.

- The gauge couplings contribute negatively to the beta function, increasing the stability. In particular, λ_{SO} is strongly stabilised.
- In the limit $\lambda_S \to 0$, λ_T completely decouples from the other Yukawa couplings.
- The perturbativity of the coupling λ_S will be critical as: (1) the gauge couplings and top Yukawa already give a positive contribution ~ 1.1 to its beta function; (2) all the other Yukawas feed into its beta function and conversely λ_S feeds into all the beta functions.

We have numerically constrained the initial values for λ_{SE}, λ_{SR}, λ_{SO}, λ_S and λ_T at the low scale (SUSY scale), so that they remain perturbative up to the GUT scale. We use the two-loop RGEs generated by the public code SARAH (see Refs. [66–70] and Ref. [88]).

In Fig. 5, we study the case of $\lambda_{SO} = 0$, which will be relevant for the two R-conserving scenarios $\mathbf{R_a}$ and $\mathbf{R_b}$. The perturbativity bounds are shown in the planes λ_S/λ_{SE} and λ_S/λ_T. As expected, we obtain the strongest constraints for λ_S, especially in the large λ_{SE} case, which is the one of interest in this paper. Furthermore, we recover that for $\lambda_S \to 0$, λ_T is insensitive to the other Yukawa couplings. Adding the parameter λ_{SO} further constrains the Yukawa couplings. This is shown in Fig. 6 where we present the perturbativity bounds on λ_{SE} and λ_{SO} for various values of λ_S and λ_T. We see that for $\lambda_{SO} \sim 0.65$, one should take $\lambda_{SE} < 0.65$ to be safely perturbative. Furthermore, as expected from the one-loop beta functions, λ_{SO} has an increased stability thanks to the strong gauge coupling contribution, allowing values up to 1.4 for low λ_{SE}. Notice in the right-hand plot of Fig. 6 that in the limit $\lambda_S \to 0$, we recover that λ_T decouples from the other Yukawas.

4.5. *Vacuum stability*

We now turn to the constraints from vacuum stability; since we have significant trilinear scalar couplings then this is of crucial importance. The tree-level scalar potential can be decomposed into four main contributions:

$$V = V_g + V_W + V_{\text{soft}} + V_{\text{hard}} \,, \tag{4.21}$$

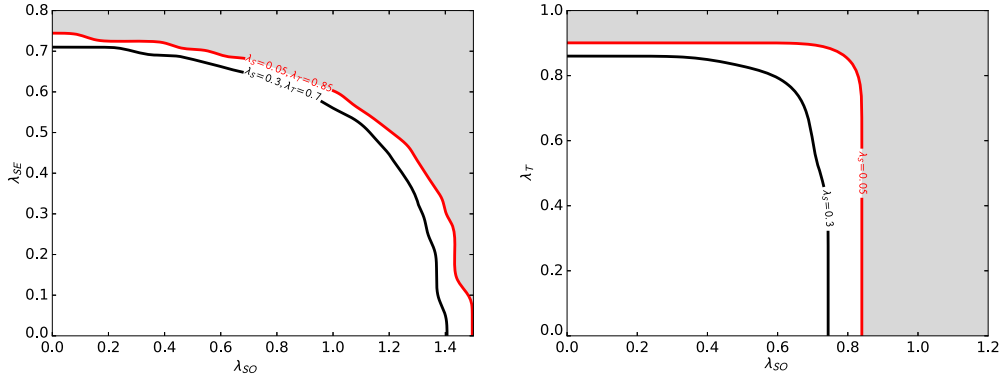

Fig. 6. Perturbativity bounds on our model around the first benchmark point from Table 3, obtained from the requirement that no couplings overtake $\sqrt{4\pi}$ before the GUT scale. We consider $\lambda_{SR} = \lambda_{SE}$. Left plot: in the $\lambda_{SO}/\lambda_{SE}$ plane with from left to right ($\lambda_S = 0.3, \lambda_T = 0.7$) and ($\lambda_S = 0.05, \lambda_T = 0.85$); all points above the curves are excluded. Right plot: in the λ_{SO}/λ_T plane with from left to right ($\lambda_S = 0.3, \lambda_{SE} = 0.65$) and ($\lambda_S = 0.05, \lambda_{SE} = 0.65$); all points above the curves are excluded.

with V_g, containing the D-term contributions, V_W the superpotential contributions and V_{soft} the soft SUSY-breaking terms. The final term V_{hard} consists of "hard" dimensionless quartic terms that are generated at the SUSY-breaking scale and look like hard SUSY-breaking terms discussed in section 3.

We have

$$V_g = \frac{1}{2}D_1^2 + \frac{1}{2}D_{2a}D_2^a + \frac{1}{2}D_{3a}D_3^a$$

where

$$D_1 = -2m_{1D}S_R + D_Y^{(0)} \qquad \text{with} \qquad D_Y^{(0)} = -g'\sum_j Y_j\varphi_j^\dagger\varphi_j$$

$$D_2^a = -\sqrt{2}m_{2D}(T^a + T^{a\dagger}) + D_2^{a(0)} \qquad \text{with} \qquad D_2^{a(0)} = -g_2\sum_j \varphi_j^\dagger M_j^a\varphi_j$$

$$D_3^a = -\sqrt{2}m_{3D}(O^a + O^{a\dagger}) + D_3^{a(0)} \qquad \text{with} \qquad D_3^{a(0)} = -g_3\sum_j \varphi_j^\dagger M_j^a\varphi_j\ ,$$

where φ_j are the scalar components of the matter chiral superfields, possibly in the adjoint representation and M_j^a is the matrix of the gauge representation of φ_j. Let us leave aside the triplet contribution (we are considering a heavy triplet and therefore expect a near-zero VEV for it) and focus on the singlet and octet terms. Similarly, we will leave aside the squarks contribution as we are not considering large A terms and therefore do not expect them to acquire a colour-breaking VEV. We have then

$$D_1^{(0)} = -\frac{g'}{2}(R_u^\dagger R_u - R_d^\dagger R_d) - g'(|\hat{E}_i|^2 - |\hat{E'}_i|^2)$$

$$D_2^{a(0)} = -g_2(R_u^\dagger\frac{\sigma^a}{2}R_u + R_d^\dagger\frac{\sigma^a}{2}R_d)$$

$$D_3^{a(0)} = -g_3 O_b^\dagger(T^a)^{bc}O_c\ ,$$

with $(T^a)^{bc} = (-if^{abc})$ and f^{abc} the $SU(3)$ structure constants.

We now turn to the superpotential contributions (we suppress the i indices for $\hat{E'}_i$ and $\hat{E'}_j$ and the "$\cdot$" denotes $SU(2)$ indices contraction by ϵ tensors) and find:

$$\begin{aligned} V_W &= \mu_r^2(R_u^\dagger R_u + R_d^\dagger R_d) + \mu_E^2(|\hat{E}|^2 + |\hat{E}'|^2) \\ &\quad + \lambda_{SE}^2\left[|\hat{E}'\hat{E}|^2 + |S|^2(|\hat{E}|^2 + |\hat{E}'|^2)\right] + \lambda_{SR}^2\left[|R_u \cdot R_d|^2 + |S|^2(|R_u|^2 + |R_d|^2)\right] \end{aligned}$$

The only "hard" SUSY-breaking terms that will be of relevance to us will be a quartic octet coupling:

$$V_{\text{hard}} \equiv \frac{\lambda_O}{4}|O^a|^4 + \lambda_{SO}^H|S|^2|O^a|^2 \tag{4.22}$$

which is of course not the only such possible term but is the most important.

After adding the soft and hard SUSY-breaking terms, we obtain

$$V = V_E + V_{SE} + V_{SR} + V_S + V_R + V_O + V_{SO}\ , \tag{4.23}$$

with

$$\begin{aligned} V_E &= (m_{\hat{E}}^2 + \mu_E^2)|\hat{E}|^2 + (m_{\hat{E}'}^2 + \mu_E^2)|\hat{E}'|^2 + \lambda_{SE}^2|\hat{E}'\hat{E}|^2 + \frac{g'^2}{2}(|\hat{E}|^2 - |\hat{E}'|^2)^2 \\ &\quad + B_E(\hat{E}\hat{E}' + h.c.) \\ V_S &\supset m_S^2|S|^2 + 2m_{1D}^2 S_R^2 + \frac{1}{2}B_S(S^2 + h.c.) \\ V_R &\supset (m_R^2 + \mu_r^2)(R_u^\dagger R_u + R_d^\dagger R_d) + \lambda_{SR}^2|R_u \cdot R_d|^2 + B_R(R_u \cdot R_d + h.c.) \\ &\quad + \frac{1}{8}\left[{g_Y}^2\,(R_u^\dagger R_u - R_d^\dagger R_d)^2 + g_2^2(R_u^\dagger \frac{\sigma^a}{2} R_u + R_d^\dagger \frac{\sigma^a}{2} R_d)^2\right] \\ V_O &\supset 2m_O^2 \text{tr}(O^\dagger O) + 2m_{3D}^2 \text{tr}(O_R^\dagger O_R) + (B_O \text{tr}(OO) + h.c.) \\ &\quad + \frac{g_3^2}{2}\left[(O_b^\dagger (T^a)^{bc} O_c)(O_b^\dagger (T_a)^{bc} O_c)\right] + \sqrt{2}g_3 m_{3D}(O + O^\dagger)^a O_b^\dagger (T_a)^{bc} O_c \\ &\quad + (T_O \text{tr}(O^3) + h.c.) + \frac{\lambda_O}{4}|O^a|^4\ , \end{aligned} \tag{4.24}$$

and the mixed contributions

$$\begin{aligned} V_{SE} &= 2{g_Y} m_{1D} S_R(|\hat{E}|^2 - |\hat{E}'|^2) + \lambda_{SE}^2|S|^2(|\hat{E}|^2 + |\hat{E}'|^2) + T_{SE}(S\hat{E}\hat{E}' + h.c.) \\ V_{SR} &= {g_Y} m_{1D} S_R(R_u^\dagger R_u - R_d^\dagger R_d) + \lambda_{SR}^2|S|^2(R_u^\dagger R_u + R_d^\dagger R_d)^2 + T_{SR}(SR_u \cdot R_d + h.c.) \\ V_{SO} &= T_{SO}(S\text{tr}(OO) + h.c.) + \lambda_{SO}^H|S|^2|O^a|^2\ . \end{aligned}$$

4.5.1. Charge-breaking minima

First, we investigate the S, $\hat{E}$, $\hat{E}'$ sector, which can drive charge-breaking minima when they all acquire a vev. The relevant tadpoles (for just one pair of $\hat{E}$, $\hat{E}'$) are

$$\begin{aligned} \frac{\partial V}{\partial \overline{S}} &\simeq m_S^2 S + \overline{B}_S \overline{S} + m_{1D}^2(S + \overline{S}) + {g_Y}\sqrt{2}m_{1D}(|\hat{E}|^2 - |\hat{E}'|^2) + \lambda_{SE}^2 S(|\hat{E}|^2 + |\hat{E}'|^2) \\ &\quad + T_{SE}\hat{E}\hat{E}' \\ \frac{\partial V}{\partial \overline{\hat{E}}} &= \hat{E}(m_{\hat{E}}^2 + \mu_E^2 + \lambda_{SE}^2|S|^2 + {g_Y} m_{1D} S_R) + \hat{E}'(B_E + T_{SE}S) + \lambda_{SE}^2\hat{E}|\hat{E}'|^2 \\ &\quad + {g_Y}^2\hat{E}(|\hat{E}|^2 - |\hat{E}'|^2) \end{aligned}$$

$$\frac{\partial V}{\partial \hat{E}'} = \hat{E}'(m^2_{\hat{E}'} + \mu^2_E + \lambda^2_{SE}|S|^2 - g_Y m_{1D} S_R) + \hat{E}(B_E + T_{SE} S) + \lambda^2_{SE}\hat{E}'|\hat{E}|^2 - g_Y{}^2 \hat{E}'(|\hat{E}|^2 - |\hat{E}'|^2)\,. \tag{4.25}$$

The study of the vacuum space of the model is divided into two regimes depending on the size of m_{1D}: relevant for this paper is the case that m_{DY} is not large, in which case the most dangerous direction is the "classic" D-flat direction $|\hat{E}|^2 = |\hat{E}'|^2$. When $S, \hat{E}, \hat{E}'$ develop vevs, we can decompose the complex fields into real and imaginary parts; without loss of generality we can put $\hat{E} = \hat{E}' \equiv \frac{1}{\sqrt{2}} E_R$, $S = \overline{S} \equiv \frac{1}{\sqrt{2}} s_R$. Solving then the equation for the singlet tadpole, we find the potential

$$V\big|_{s_R} = \frac{E_R^2}{4(\lambda^2_{SE} E_R^2 + m^2_{SR})}\Bigg[\lambda^4_{SE}\Big(E_R^2 + \frac{1}{2}\big(2m^2_{ER} + m^2_{SR} - \hat{T}^2_{SE}\big)^2 - \frac{1}{4}\Big(\hat{T}^4_{SE} - 2\hat{T}^2_{SE}(m^2_{SR} + 2m^2_{ER}) + (m^2_{SR} - 2m^2_{ER})^2\Big)\Bigg] \tag{4.26}$$

where we defined

$$\begin{aligned} \hat{T}_{SE} &\equiv T_{SE}/\lambda_{SE} \\ m^2_{SR} &\equiv m^2_S + B_S + 4m^2_{DY} \\ m^2_{ER} &\equiv m^2_{\hat{E}} + m^2_{\hat{E}'} + 2B_E + 2\mu^2_E. \end{aligned} \tag{4.27}$$

Clearly we observe that we have appearance of a charge-breaking vacuum if

$$\frac{T^2_{SE}}{\lambda^2_{SE}} > 2m^2_{ER} + m^2_{SR}\,. \tag{4.28}$$

However, it is only lower than our vacuum if the weaker condition

$$\frac{T^2_{SE}}{\lambda^2_{SE}} > 2m^2_{ER} + m^2_{SR} + 2\sqrt{2} m_{ER} m_{SR} \tag{4.29}$$

is satisfied, or equivalently

$$m_{ER} < \frac{1}{\sqrt{2}}\Big(\frac{T_{SE}}{\lambda_{SE}} - m_{SR}\Big). \tag{4.30}$$

The analogous constraints also apply for the pseudoscalar direction, and also for the S, R_u, R_d sector.

4.5.2. Colour-breaking minima

A crucial part of our analysis is the presence of trilinear couplings of the singlet to the octet, which generate a coupling to gluons. However, just as the couplings to the selectron-like states allow charge-breaking minima, the octet scalar couplings permit colour-breaking minima. The analysis is identical for O_R or O_I with the opposite sign for T_{SO}, so let us choose O_R. The tadpole equations read

$$\begin{aligned} 0 &= (m^2_S + \frac{1}{2}\lambda^H_{SO} O_R^2 + \frac{1}{2}\lambda^2_{SO} O_R^2) s_R - \frac{O_R^2 T_{SO}}{2\sqrt{2}} \\ 0 &= O_R\Big(m^2_{OR} + \frac{\lambda_O + \lambda^2_{SO}}{4} O_R^2 + \frac{1}{2}(\lambda^H_{SO} + \lambda^2_{SO}) s_R^2 - \frac{1}{\sqrt{2}} T_{SO} s_R\Big) \end{aligned} \tag{4.31}$$

where now $m_{OR}^2 \equiv m_O^2 + B_O + 4|m_{D3}|^2$. We therefore see that the supersymmetric terms are equivalent to putting $\lambda_O = \lambda_{SO}^2$, $\lambda_{SO}^H = \lambda_{SO}^2$; in an analysis identical to the previous subsection we find that an additional vacuum exists when

$$T_{SO}^2 > (\lambda_O + \lambda_{SO}^2) m_{SR}^2 + 4(\lambda_{SO}^H + \lambda_{SO}^2) m_{OR}^2, \tag{4.32}$$

but that the minimum is only lower than the colour-preserving one when

$$T_{SO}^2 > \left(2\sqrt{\lambda_{SO}^H + \lambda_{SO}^2}\, m_{OR} + \sqrt{\lambda_O + \lambda_{SO}^2}\, m_{SR}\right)^2, \tag{4.33}$$

or equivalently, when $\lambda_{SO} \neq 0$,

$$m_{OR} < \frac{1}{2\sqrt{\lambda_{SO}^H + \lambda_{SO}^2}} \left(T_{SO} - m_{SR}\sqrt{\lambda_O + \lambda_{SO}^2}\right). \tag{4.34}$$

If we choose to break R-symmetry only in the Higgs sector via a B_μ-term, then $\lambda_{SO} = 0$. In this case, we need to rely on λ_{SO}^H and λ_O only to stabilise the potential, leading to very strong constraints on the trilinear T_{SO}. For instance, if we have $\lambda_{SO}^H, \lambda_O \sim \mathcal{O}(0.04)$ and a 400 GeV scalar octet, the trilinear T_{SO} must be smaller than 310 GeV to ensure that the colour-preserving vacuum is stable.

5. Finding a di-photon excess in the MDGSSM

5.1. Prelude

While the MDGSSM has a large set of free parameters, the most relevant ones can be divided into three roughly independent sets controlling different features:

1. **Higgs and singlet masses and mixing**: m_{1D}, m_S, B_S, $\tan\beta$, μ, λ_S and λ_T.
2. **Singlet decay/production amplitude to** gg: $T_{SO}, m_O, B_O, m_{\tilde{q}}$, where $m_{\tilde{q}}$ is the soft masses for right (or left)-handed squarks.
3. **Singlet decay amplitude to** $\gamma\gamma$: $T_{SE}, T_{SR}, \lambda_{SR}, \lambda_{SE}$ supplemented with soft masses and B terms for the fields $\hat{E}$, $\hat{E}'$, R_u and R_d.

The first set is dedicated to reproducing the measured Higgs boson mass as well as a 750 GeV scalar singlet. The value of λ_S need to be adjusted to have a small mixing between both scalars, which is necessary both for the diphoton cross-section and for having $m_H \in [122, 128]$. The second set can be then used to enhance the production rate of singlet through gluon fusion. The trilinears T_{SO} are crucial in this respect as they allow the scalar octet to participate in the loop-induced coupling Sgg, greatly increasing the singlet production rate. Finally, the last set of parameters is used to increase the diphoton amplitude. The superpotential Yukawa couplings λ_{SE} and λ_{SR} from (2.4) are constrained to be below 0.7 to avoid the appearance of Landau poles before the GUT scale. The trilinears are mainly constrained by enforcing that the scalar fields $\hat{E}$, $\hat{E}'$, R_u and R_d does not get a charge-breaking vacuum expectation value.

We will investigate various scenarios that we can classify according to the presence or not of the R-violating terms (2.5):

- R-symmetry preserving models (modulo, as discussed in section 2, a B_μ-term), which do not include the terms (2.5) and have R-charges for the fake leptons such that only the superpotential couplings λ_E and λ_{SR} to S are allowed. We distinguish the models

  - $\mathbf{R_a}$: where we will consider large Dirac mass m_{1D}, so that the coupling to gluons proceeds through squarks loops.
  - $\mathbf{R_b}$: where instead consider small Dirac masses but light scalar octet, so that the coupling to gluons proceeds through scalar octet loops.
- R-symmetry violating models, for which we can have additionally the terms (2.5) and the trilinears T_{SE} and T_{SR}. We consider
  - $\not{\mathbf{R}}_a$: A generalisation of scenario $\mathbf{R_a}$ with λ_{SO} and the trilinears T_{SE} and T_{SR} included.
  - $\not{\mathbf{R}}_b$: Similar to the model $\not{\mathbf{R}}_a$, but we further tolerate the presence of a Majorana gauginos mass terms. This allows to simultaneously produce the scalar S_R and pseudo-scalar S_I singlet and have a "double-peaks" resonance set-up.

In the following we shall present results of a numerical investigation of the parameter space of the MDGSSM for various scenarios. To do this we used the package `SARAH` to produce `SPheno` code to calculate the spectrum, production rate and decays. We created a new model file for the MDGSSM including the adjoint couplings λ_{SO}, T_{SO}. However, we found that modifications to the `SPheno` code were necessary:

1. We use pole masses instead of $\overline{\text{DR}}$-masses for the selectrons and octet scalars in the calculation of loop couplings with the neutral scalars. This is because these masses are the most important for the gluon and photon couplings of our 750 GeV candidate, and can differ by more than a factor of two; as described in [11], using the $\overline{\text{DR}}$ masses is less accurate and so we employ pole masses just for these particles.
2. To facilitate our search for valid parameter points, we produced two different versions of the code. The first solves the tadpole equations for mass-squared parameters $m^2_{H_u}, m^2_{H_d}, m^2_S, m^2_T$ taking v_S, v_T as inputs; while this is the appropriate choice for implementing the loop corrections to the scalar masses correctly, it is, however, difficult to choose the vacuum expectation values v_S, v_T (since loop corrections can rapidly change the values of m^2_S, m^2_T by several orders of magnitude). We therefore use this version of the code to check the results of our second code, which was specially modified to first solve the two-loop tadpole equations numerically for v_S, v_T, and then compute the tadpoles and masses using these values as inputs, solving for m^2_S, m^2_T again along the same lines as the first code. While this is computationally expensive (computing the two-loop corrections to the neutral scalar tadpoles twice for each point) it is the most efficient way to correctly identify points – and not miss points where, for example, m^2_S may be identified as tachyonic at "tree level".

5.2. R-Symmetry conserving Scenarios

Consider first the scenarios $\mathbf{R_a}$ and $\mathbf{R_b}$ where we include only the R-symmetry conserving adjoint couplings. Under these constraints, the singlet production proceeds mainly by gluons fusion through loops of squarks (controlled by $g_Y m_{1D}$) and (pseudo-)scalar octets (controlled by the trilinear T_{SO}).

5.2.1. Squark-induced gluon fusion

We start with scenario $\mathbf{R_a}$ and present in Table 2 a benchmark point satisfying all the previously-mentioned constraints while retaining a sizeable $\gamma\gamma$ cross-section.

Table 2
Benchmark point for our scenario. We further have, $B_\mu = 2.5^2$ TeV^2, the heavy left-handed squarks (as well as right-handed sbottom) have masses around 2.25 TeV. The two first generation of right-handed squarks have masses at 975 GeV (**R**$_\mathbf{a}$) or 1300 GeV (**R**$_\mathbf{b}$), left-handed sleptons have masses at 1.5 TeV. We have $m_{2D} = 1200$ GeV (**R**$_\mathbf{a}$) or 900 GeV (**R**$_\mathbf{b}$), and $m_{3D} = 2.5$ TeV (**R**$_\mathbf{a}$) or 3 TeV (**R**$_\mathbf{b}$).

	Parameter	**R**$_\mathbf{a}$	**R**$_\mathbf{b}$
Higgs mass	μ	925 GeV	450 GeV
	$\tan\beta$	3	5
	λ_T	0.7	0.85
	$\sqrt{m_T^2}$	500 GeV	1000 GeV
Singlet masses and mixing	m_{1D}	1250 GeV	100 GeV
	$\sqrt{m_S^2}$	500 GeV	775 GeV
	B_S	-2.44^2 TeV^2	-200^2 GeV^2
	λ_S	0.29	0.05
Singlet decay/production amplitude to gg	T_{SO}	200 GeV	300 GeV
	$\sqrt{m_O^2}$	1300 GeV	1025 GeV
	$m_{\tilde{t}_R}$	500 GeV	1200 GeV
Singlet decay amplitude to $\gamma\gamma$	$\lambda_{SR} = \lambda_{SE}$	0.7	0.7
	$m_E^2 = m_{R_{u,d}}^2$	10^2 GeV^2	150^2 GeV^2
	$\mu_E = \mu_{R_{u,d}}/1.4$	325 GeV	65 GeV
	$m_{\tilde{l}R}$	250 GeV	500 GeV
Outputs	Pole mass Higgs	125.5 GeV	124.9 GeV
	Pole mass S_R	750.1 GeV	755.7 GeV
	Pole mass O_I/O_R (**R**$_\mathbf{a}$/**R**$_\mathbf{b}$)	945.5 GeV	390.0 GeV
	Pole mass $\tilde{t}_R$	820.3 GeV	1165.0 GeV
	Pole mass $\tilde{l}_R$	418 GeV	513 GeV
	Pole mass $\tilde{\tilde{E}}$	397 GeV	382 GeV
	$\sigma(S_R \to \gamma\gamma)$	**3.20 fb**	**3.18 fb**
	$\Delta\rho$	0.97×10^{-4}	3.17×10^{-4}
	v_S	151.4 GeV	643.5 GeV

The main aspects of this scenario are the following:

- We limit the R-symmetry breaking to the Higgs sector, and therefore choose R-charge of the fake fields to allow $\lambda_{SE}, \lambda_{SR}$ superpotential terms but not trilinears T_{SE}/T_{SR} and the corresponding B-terms.
- The loop coupling to gluons will proceed through squark loops, with singlet/squarks coupling enhanced by a large Dirac mass m_{1D}.
- The loop coupling to photons have numerous contributions through loops of fake fields (both fermions and scalars) and sleptons.
- Finally, because of the large Dirac mass, one need a sizeable negative B_S to ensure that the scalar singlet has a mass of 750 GeV.

Notice that a satisfying feature of this scenario is that we do not need to fine-tune the mass of the fields participating in the loop coupling between S and $\gamma\gamma$.

Regarding the scalar singlet production, gluon fusion proceeds mainly through loops of 800 GeV right-handed stop and TeV right-handed first two squarks generations, while left-

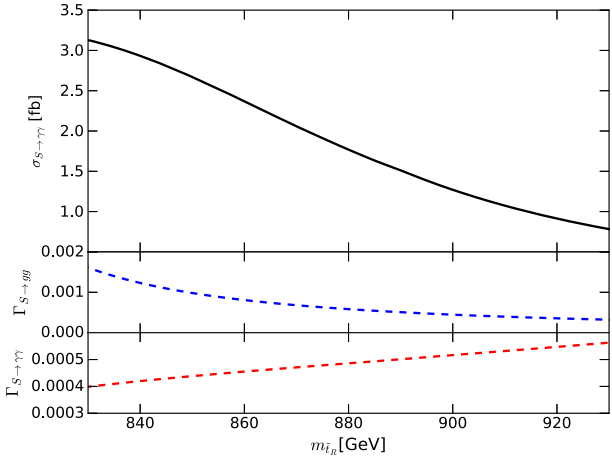

Fig. 7. $S_R \to \gamma\gamma$ cross section in fb as a function of the one-loop mass for the right-handed squarks. The lower two parts show the amplitudes to $\gamma\gamma$ and to gg.

handed squarks are heavier at 1.75 TeV. As a consequence, the mass of the right-handed stop is a critical parameter in enhancing $\sigma_{\gamma\gamma}$, we illustrate this dependence in Fig. 7 where we plot the $S_R \to \gamma\gamma$ cross-section as a function of the stop one-loop mass, by varying around the benchmark point of Table 2. We see that the cross-section decreases very rapidly with the stop mass.

Regarding the scalar singlet decay to diphoton, it proceeds both through loops of light right-handed sleptons (we consider left-handed sleptons above the TeV) controlled by $g_Y m_{1D}$ and loops of fake leptons, $\hat{E}$, $\hat{E}'$, R_u and R_d which are controlled by a unified Yukawa $\lambda_{SR} = \lambda_{SE} = 0.7$. Furthermore, the fake sleptons also contribute with couplings controlled by $g_Y m_{1D}$. In order to maximise the overall contribution, one has to take care that no cancellations occur between the various contributions (particularly for the D-term-induced couplings, which are proportional to the hypercharge of the scalar participating in the loop). Referring to Table 1 we see that one possible choice is light $\hat{E}$, R_d and right-handed sleptons and heavier $\hat{E}'$, R_u and left-handed sleptons.

In order to have sizable contributions from the (fake) sleptons, we need a reasonably large singlet Dirac mass $m_{1D} \sim 1250$ GeV, this has the added benefit that it also enhances the squark contributions to the scalar singlet production rate. On the other hand, it increases the tuning of λ_S necessary to have a small mixing and additionally implies that we have either a small $\tan\beta$ or a somewhat large μ term as can be seen from Eq. (4.6).

Overall, Fig. 8 presents the cross-section obtained in the λ_S/μ_E plane by varying around the benchmark point of Table 2. Roughly speaking, this figure combines on the abscissa the constraints from mixing with on the ordinate the requirement that the particles participating in the loop have masses close to half that of the resonance.[7]

We see from Fig. 8 that the main requirement in our model is that we must consider values of λ_S tuned at the level of a few percent. We can see that the constraint from the ratio $\Gamma_{ZZ}/\Gamma_{\gamma\gamma}$ is significantly weaker than the requirement on the cross-section.

[7] Notice that the fake lepton mass obtains a sizeable contribution from the vev of S through the λ_{SE} term.

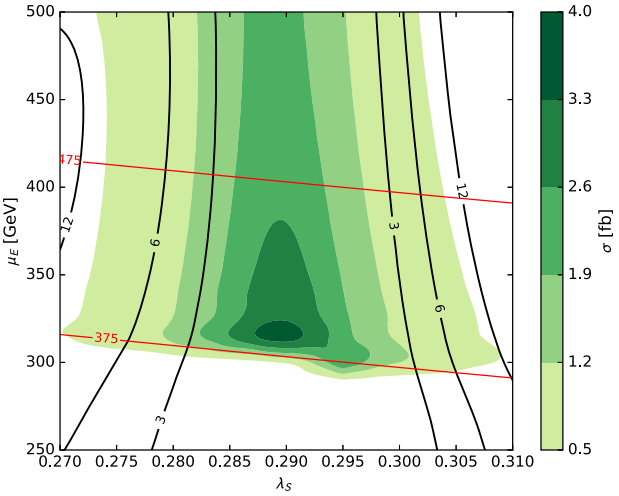

Fig. 8. $S_R \to \gamma\gamma$ cross section in fb as a function of the μ_E and λ_S. The plot is based on the benchmark point of Table 2. The black contour shows the most constraining ratio from (4.11) while the red contours shows the pole mass for the fake leptons. (For interpretation of the references to colour in this figure legend, the reader is referred to the web version of this article.)

5.2.2. *Octet-induced gluon fusion*

Let us now consider the case $\mathbf{R_b}$ where we take a light scalar octet. Following the discussion of the previous section, its mass is not constrained as long as we take a large Dirac gluino mass. We will therefore focus on $m_{3D} = 3$ TeV. Since m_{3D} contributes at tree-level in the mass of the scalar octet, we require large negative $B_O \sim -4m_{3D}$ in order to have it close to the resonant mass of 375 GeV. While this is a new source of tuning, the fact that the scalar octet provides a sufficient coupling between the gluons and singlet means that we no longer need a sizeable Dirac mass m_{1D} as in $\mathbf{R_a}$. As a consequence, the tuning on λ_S is milder in this scenario, as can be seen from Fig. 9. We have presented in Table 2 a benchmark point for this scenario.

As the singlet Dirac mass is small, the sleptons do not contribute to the singlet decay to diphotons, in stark contrast with scenario $\mathbf{R_a}$. One relies on loops of fake (s)leptons to increase $\sigma_{S_R\to\gamma\gamma}$. The crucial parameter in this model is therefore the fake leptons mass, as we illustrate in Fig. 9.

5.3. *R-Symmetry violating scenarios*

Although we have successfully demonstrated in the previous section that we are able to explain the di-photon excess in the MDGSSM with an R-preserving SUSY-breaking sector, we would like to discuss as well two interesting R-violating scenarios. While in the first scenario, the scalar singlet remains the resonant particle, we allow for a Majorana gaugino mass in the second scenario, leading to the possibility of having the scalar and pseudo-scalar singlet almost degenerate in mass.

5.3.1. *Scenario $\not{\mathbf{R}}_{\boldsymbol{a}}$: allowing for λ_{SO} and T_{SE}, T_{SE}*

When allowing for R-violation beyond the Higgs sector, the most obvious and minimal choice is to allow for the trilinear terms

$$-\Delta\mathcal{L}^{\text{scalar soft}}_{\text{vector-like}} \supset [T^{ij}_{SE} S\hat{E}_i \hat{E}'_j + T_{SR} S R_d R_u + h.c.] \tag{5.1}$$

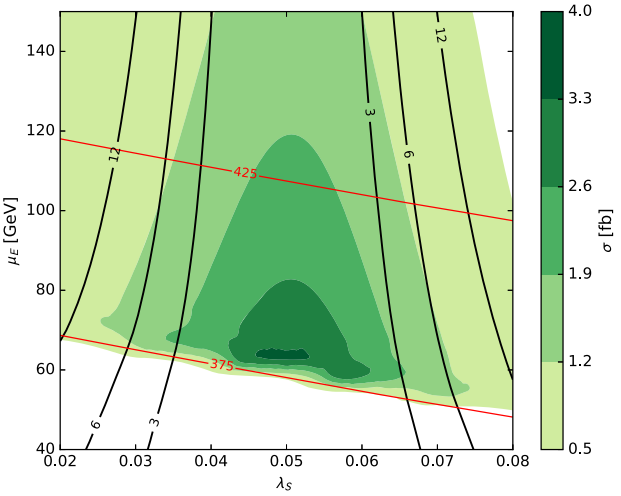

Fig. 9. $S_R \to \gamma\gamma$ cross section in fb as a function of the μ_E and λ_S for scenario $\mathbf{R_b}$. The plot is based on the benchmark point of Table 2. The black contour shows the most constraining ratio from (4.11) while the red contours shows the pole mass for the fake leptons. (For interpretation of the references to colour in this figure legend, the reader is referred to the web version of this article.)

and

$$W_{RV} \supset \lambda_{SO}\mathbf{S}\mathrm{tr}(\mathbf{OO}) \tag{5.2}$$

leading to a stabilising quartic contribution. When introducing the former, upper limits on the trilinear couplings T_{SE} and T_{SR} have to be taken into account in order to ensure the absence of a (lower) charge breaking minimum. The introduction of the quartic with λ_{SO}, however, contributes to stabilising the potential to prevent colour breaking minima and thus allows a further increase in T_{SO} (cf. Sec. 4.5) which in turn leads to an enhancement of the partial decay width of $\Gamma_{S\to gg}$. As indicated in Eq. (4.33) the upper limit on T_{SO} is mainly constrained by the size of the Yukawa coupling λ_{SO}. As we require perturbativity up to the GUT scale, λ_{SO} itself is limited, as studied in detail in Sec. 4.4. Taking $\lambda_S \approx 0.3$ and $\lambda_T \approx 0.7$ (the latter being motivated to be larger to obtain the correct Higgs mass) the size of the Yukawa couplings $\lambda_{SE} = \lambda_{SR}$ and λ_{SO} are naturally constrained. Generally, moderate values for both Yukawa couplings are of interest in order to provide sizable couplings in the photon and gluon partial decay widths. As demonstrated in Fig. 6, right plot, we can choose $\lambda_{SE} = \lambda_{SO} = 0.65$, while still being perturbative up to the high scale. This in turn implies that a trilinear $T_{SO} = 1.5$ TeV is still in concordance with vacuum stability, in contrast to the previously studied scenario $\boldsymbol{R_a}$, where a maximal value of 200 GeV was possible. With respect to charge breaking minima, we have checked that $T_{SE} = -1$ TeV does not lead to charge breaking minima within our Benchmark Scenario $\not{\boldsymbol{R}}_{\boldsymbol{a}}$, whose further parameters are given in Table 3.

By including those new R-violating terms, we open up further interesting regions in parameter space leading to an enhanced di-photon signal. For illustration we refer to Fig. 10, where the cross section $\sigma(gg \to S \to \gamma\gamma)$ is shown in dependence of the trilinears T_{SO} and $T_{SE} = T_{SR}$. In red and black solid lines, the partial widths $\Gamma_{S\to\gamma\gamma}$ and $\Gamma_{S\to gg}$ are depicted in units of $\times 10^{-5}$ GeV. As can be seen, the increase of T_{SO} enhances the partial decay width of $\Gamma_{S\to gg}$, as it increases the coupling of the pseudo-scalar octets ($m_{\sigma_0} = 886.30$ GeV) in the loop to the singlet. However, this effect is reduced by an increase of the octet mass via loop effects. At the same time, the

Table 3
Overview of the input parameters, physical masses, constraints and signal cross section for both R-violating scenarios $\not{R}_a$ and $\not{R}_b$.

Parameter	$\not{R}_a$	$\not{R}_b$
$\tan\beta$	2	4
μ	660 GeV	450 GeV
B_μ	2500 GeV	2500 GeV
$\sqrt{m_S^2}$	490 GeV	310 GeV
B_S	-2.4^2 TeV^2	-0.7^2 TeV^2
$\sqrt{m_T^2}$	1250 GeV	1200 GeV
$\sqrt{m_O^2}$	530 GeV	890 GeV
M_3	0	1400 GeV
m_{1D}	1250 GeV	490 GeV
m_{2D}	1000 GeV	1000 GeV
m_{3D}	1600 GeV	2300 GeV
λ_S	0.29	0.27
λ_T	0.65	0.70
λ_{SO}	0.65	0.65
$\lambda_{SR} = \lambda_{SE}$	0.65	0.65
$T_{SE} = T_{SR}$	-1000 GeV	0 GeV
T_{SO}	1500 GeV	600 GeV
$M_{\tilde{Q}}$	2000 GeV	2000 GeV
$M_{\tilde{u}}$	1700 GeV	1500 GeV
$M_{\tilde{d}}$	2000 GeV	2000 GeV
$M_{\tilde{L}}$	1500 GeV	1500 GeV
$M_{\tilde{e}}$	820 GeV	700 GeV

Parameter	$\not{R}_a$	$\not{R}_b$
$\mu_E = \mu_{R_{u,d}}$	413 GeV	250 GeV
$m^{11\,2}_{\hat{E}} = m^{22\,2}_{\hat{E}}$	400^2 GeV^2	400^2 GeV^2
$m^{11\,2}_{\hat{E}'} = m^{22\,2}_{\hat{E}'}$	600^2 GeV^2	400^2 GeV^2
$m^2_{\hat{R}_u}$	600^2 GeV^2	400^2 GeV^2
$m^2_{\hat{R}_d}$	400^2 GeV^2	400^2 GeV^2
$B^{11}_{\hat{E}} = B^{22}_{\hat{E}} = B_{\hat{R}}$	88500	22200
m_h	124.8 GeV	125.9 GeV
m_{S_R}	755.7 GeV	756.5 GeV
m_{S_I}	1125.1 GeV	751.0 GeV
m_{σ_0}	886.3 GeV	886.3 GeV
$m_{\tilde{e}}$	382.2 GeV	386.7 GeV
m_e	378.6 GeV	377.2 GeV
$m_{\tilde{u}}$	1776.5 GeV	1597.2 GeV
$m_{\tilde{g}}$	1825.8 GeV	1916.0 GeV
$\Gamma_{S\to ZZ}/\Gamma^{\rm obs}_{S\to\gamma\gamma}$	0.1	0.0
$\Gamma_{S\to hh}/\Gamma^{\rm obs}_{S\to\gamma\gamma}$	0.5	1.2
$\Gamma_{S\to WW}/\Gamma^{\rm obs}_{S\to\gamma\gamma}$	0.3	0.0
$\Gamma_{S\to gg}/\Gamma^{\rm obs}_{S\to\gamma\gamma}$	0.7	4.4
$\Delta\rho$	9.9×10^{-5}	2.4×10^{-4}
$\sigma(S_R\to\gamma\gamma)$	**3.1 fb**	**4.4 fb**

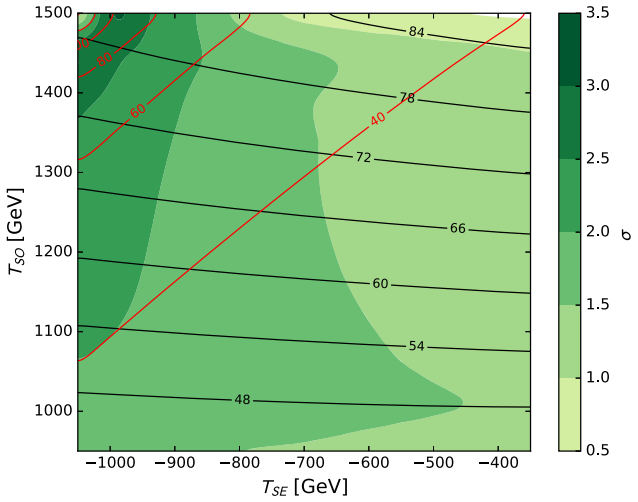

Fig. 10. Variation of $T_{SE} = T_{SR}$ and T_{SO} while taking the remaining parameters fixed as in benchmark scenario $\not{R}_a$. $\Gamma_{S\to\gamma\gamma}$ and $\Gamma_{S\to gg}$ are depicted in units of $\times10^{-5}$ GeV in red and black solid lines, respectively. The green shaded areas show the signal cross section $\sigma(gg\to S\to\gamma\gamma)$ in fb. (For interpretation of the references to colour in this figure legend, the reader is referred to the web version of this article.)

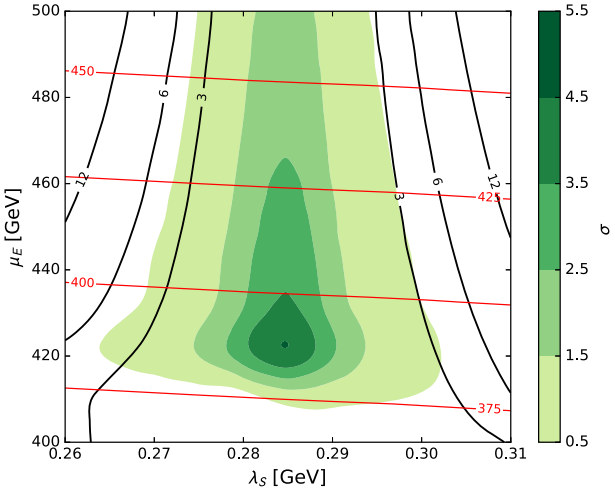

Fig. 11. λ_S–μ_E plane for benchmark scenario $\not{R}_a$. In red solid lines the mass of the lightest fake leptons are shown, the black solid lines indicate $\Gamma_{S\to ZZ}/\Gamma_{S\to\gamma\gamma}$. The green shaded areas indicate the signal cross section $\sigma(gg \to S \to \gamma\gamma)$ in fb. (For interpretation of the references to colour in this figure legend, the reader is referred to the web version of this article.)

increase of T_{SO} leads as well to a decrease of the mass of the fake sleptons, which increases the partial decay width of $\Gamma_{S\to\gamma\gamma}$. The production via squarks ($m_{\tilde{q}} > 1.7$ TeV) is suppressed in this scenario. A further enhancement of $\Gamma_{S\to\gamma\gamma}$ is achieved by increasing $T_{SE} = T_{SR}$. As naively expected, the highest cross section is found for higher trilinears, such that we have chosen corresponding values ($T_{SO} = 1.5$ TeV and $T_{SE} = -1$ TeV) for our benchmark point $\not{R}_a$, which is given in more detail in Table 3. This scenario features light fake sleptons and fake electrons which are below 400 GeV thus leading, together with the large T_{SE}, to an enhanced partial decay $S \to \gamma\gamma$. Similar to the R-conserving Scenario, we account for a mass hierarchy between $\hat{E}$, R_d and $\tilde{e}^c$ and $\hat{E}'$, R_u and L to prevent cancellations from D-term induced couplings, which could still be further increased to allow for an even larger cross section. The coupling to the sfermions is further enhanced by a large Dirac mass $m_{1D} = 1250$ GeV. Choosing a large $m_{3D} = 1600$ GeV, the gluino mass lies above 1800 GeV and is safe from exclusion limits. A large $m_T = 1250$ GeV guarantees further that the $\Delta\rho$-parameter is below the current limits.

In total, this scenario features a signal cross section of $\sigma(S \to \gamma\gamma) = 3.1$ fb, and is in full agreement with further current experimental exclusion limits, e.g. limits on the ratios of $\Gamma_{S\to XX}/\Gamma^{\text{obs}}_{S\to\gamma\gamma}$ resulting from LHC8 data, as indicated in Table 3.

As for the previous scenarios, we show in Fig. 11 the λ_S–μ_E plane around the benchmark scenario. A comparable tuning of λ_S is observed as for $\not{R}_a$. It could be further relaxed when e.g. allowing for smaller m_{1D} masses. Fig. 11 demonstrates as well that the constraints from $\Gamma_{S\to ZZ}/\Gamma^{\text{obs}}_{S\to\gamma\gamma}$ are less constraining than the aimed for signal cross section.

5.3.2. Scenario $\not{R}_b$: "Double-peak" scenario

In the second R-violating scenario, we want to discuss the possibility of having a degenerate scalar and pseudo-scalar singlet. Only when the soft Majorana gaugino mass term M_3 is included, production via gluon fusion is possible and leads to a sizeable mass splitting between the Majorana gluinos. Having two particles leading to a di-photon signal, a broad parameter space opens

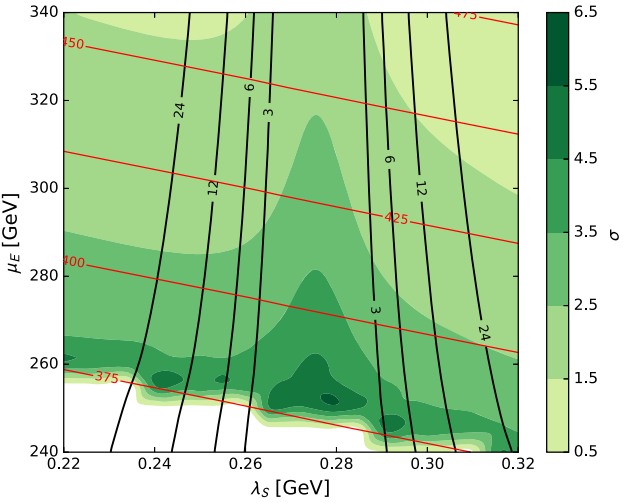

Fig. 12. λ_S–μ_E plane for benchmark scenario $\not{R}_b$. In red solid lines the mass of the lightest fake leptons are shown, the black solid lines indicate $\Gamma_{S\to ZZ}/\Gamma_{S\to\gamma\gamma}$. The green shaded areas show the cross section $\sigma(gg \to S \to \gamma\gamma)$ in fb. (For interpretation of the references to colour in this figure legend, the reader is referred to the web version of this article.)

up. As an example we have chosen $\not{R}_b$ as benchmark scenario, whose parameters are given in Table 3. For comparison with the previous scenarios we show again the λ_S–μ_E plane around the benchmark scenario, see Fig. 12. With the pseudo-scalar singlet not being constrained by mixing with the Higgs like for the scalar singlet, a large variation in λ_S is possible as with respect to the R-conserving scenarios or $\not{R}_a$. Also the smaller Dirac mass m_{1D} leads to a reduced tuning in this scenario. Besides being less tuned, we clearly demonstrate that the aimed for signal cross section (and even higher values) can be easily obtained, which could be even higher by allowing for large trilinears T_{SE}, T_{SR}, T_{SO} or a mass hierarchy between $\hat{E}$, R_d and $\tilde{e}^c$ and $\hat{E}'$, R_u and L. This clearly demonstrates that such a scenario features various possibilities of creating a sizable di-photon signal. In the chosen benchmark point, we feature, e.g., a scalar and pseudo-scalar mass of 756.5 GeV and 751.0 GeV, respectively, and a signal cross section of 4.4 fb, while still being in agreement with experimental limits like on the ratios of $\Gamma_{S\to XX}/\Gamma^{\text{obs}}_{S\to\gamma\gamma}$ from LHC8 data, $\Delta\rho$, or direct searches. Such kind of scenarios could also be able to explain a preference for a larger width as is in discussion with respect to the ATLAS analyses, for example.

Generally, these are only two of various scenarios which could be realised in case of allowing for R-violation. Again, this demonstrates that the MDGSSM is able to inherently accommodate a di-photon signal as currently observed.

6. Conclusions

The MDGSSM is promising as a model that reproduces the di-photon excess observed at both LHC experiments, ATLAS and CMS. It automatically contains a singlet with both scalar (S_R) and pseudoscalar (S_I) components that can both be at the origin of the resonance. It is quite easy to fix the mass of one or both of them at 750 GeV. In the latter case, a small splitting will simulate the larger width of the resonance for which there is a mild preference in the present ATLAS data. Also the model contains new states beyond those of the MSSM, triplets, octets and fake leptons, that can be used in the loops to generate both the production of the singlet and its

decay to photons. We have shown that there are diverse experimental constraints that are quite stringent.

We have found that if the resonance is to be identified with the scalar S_R, keeping its mixing with the Standard Model Higgs within the experimentally allowed range represents the most constraining issue. We have found that a certain amount of cancellation is needed between certain parameters and this can be translated in a tuning of the trilinear λ_S at the level of a few percent. Fortunately, this happens to values of λ_S sitting in a quite natural range, near the values expected from an $N = 2$ supersymmetric origin of the coupling.

We found that while remaining within the assumptions of the MDGSSM – perturbative couplings up to the GUT scale, R-symmetry-breaking only in the superpotential – the signal can be easily fit by including new dimensionful trilinear couplings of just the adjoints. The latter have not attracted attention in existing literature on Dirac gaugino models, despite the fact that they respect R-symmetry and so are always allowed. While they come out typically small in some scenarios of supersymmetry breaking, this is not always the case and they are expected to be present in the model. We have provided a first comprehensive discussion on this point. We then performed numerical scans of large parts of the parameter space using the most advanced tools available and in particular the most sophisticated calculation of the Higgs mass (up to two loop order). We found different regions of the parameter space of the MDGSSM (and given example benchmark points) satisfying all existing constraints while providing a good fit to the observed di-photon excess. Moreover, the relevant points have large quantum corrections (in particular to the singlet mass and vacuum expectation value) underlining the importance of using numerical tools.

Acknowledgements

The work of K.B and M.D.G is supported by the Agenge Nationale de Recherche under grant ANR-15-CE31-0002 “HiggsAutomator”. K.B also acknowledges the support of the European Research Council (ERC) under the Advanced Grant Higgs@LHC (ERC-2012-ADG20120216-321133). The work of L.D and J.H has been supported by the Labex ILP (reference ANR-10-LABX-63) part of the Idex SUPER, and received financial state aid managed by the Agence Nationale de la Recherche, as part of the programme Investissements d’avenir under the reference ANR-11-IDEX-0004-02.

References

[1] CMS Collaboration, Search for new physics in high mass diphoton events in proton–proton collisions at $\sqrt{s} =$ 13 TeV, Tech. Rep. CMS-PAS-EXO-15-004, CERN, Geneva, 2015, https://cds.cern.ch/record/2114808.

[2] Search for resonances decaying to photon pairs in 3.2 fb^{-1} of pp collisions at $\sqrt{s} = 13$ TeV with the ATLAS detector, Tech. Rep. ATLAS-CONF-2015-081. CERN, Geneva, Dec 2015, http://cds.cern.ch/record/2114853.

[3] CMS Collaboration, Search for new physics in high mass diphoton events in 3.3 fb^{-1} of proton–proton collisions at $\sqrt{s} = 13$ TeV and combined interpretation of searches at 8 TeV and 13 TeV, Tech. Rep. CMS-PAS-EXO-16-018, CERN, Geneva, 2016, https://cds.cern.ch/record/2139899.

[4] M.R. Buckley, Wide or narrow? The phenomenology of 750 GeV diphotons, arXiv:1601.04751 [hep-ph].

[5] A. Angelescu, A. Djouadi, G. Moreau, Scenarii for interpretations of the LHC diphoton excess: two Higgs doublets and vector-like quarks and leptons, Phys. Lett. B 756 (2016) 126–132, arXiv:1512.04921 [hep-ph].

[6] S. Di Chiara, L. Marzola, M. Raidal, First interpretation of the 750 GeV diphoton resonance at the LHC, Phys. Rev. D 93 (9) (2016) 095018, arXiv:1512.04939 [hep-ph].

[7] R.S. Gupta, S. Jäger, Y. Kats, G. Perez, E. Stamou, Interpreting a 750 GeV diphoton resonance, arXiv:1512.05332 [hep-ph].

[8] D. Choudhury, K. Ghosh, The LHC diphoton excess at 750 GeV in the framework of the constrained minimal supersymmetric standard model, arXiv:1605.00013 [hep-ph].
[9] A. Djouadi, A. Pilaftsis, The 750 GeV diphoton resonance in the MSSM, arXiv:1605.01040 [hep-ph].
[10] A. Bharucha, A. Djouadi, A. Goudelis, Threshold enhancement of diphoton resonances, arXiv:1603.04464 [hep-ph].
[11] F. Staub, et al., Precision tools and models to narrow in on the 750 GeV diphoton resonance, arXiv:1602.05581 [hep-ph].
[12] K. Benakli, M. Goodsell, F. Staub, W. Porod, Constrained minimal Dirac gaugino supersymmetric standard model, Phys. Rev. D 90 (4) (2014) 045017, arXiv:1403.5122 [hep-ph].
[13] P. Fayet, Massive gluinos, Phys. Lett. B 78 (1978) 417.
[14] P.J. Fox, A.E. Nelson, N. Weiner, Dirac gaugino masses and supersoft supersymmetry breaking, J. High Energy Phys. 0208 (2002) 035.
[15] M. Heikinheimo, M. Kellerstein, V. Sanz, How many supersymmetries?, J. High Energy Phys. 04 (2012) 043, arXiv:1111.4322 [hep-ph].
[16] G.D. Kribs, A. Martin, Supersoft supersymmetry is super-safe, Phys. Rev. D 85 (2012) 115014, arXiv:1203.4821 [hep-ph].
[17] G.D. Kribs, A. Martin, Dirac gauginos in supersymmetry – suppressed jets + MET signals: a snowmass whitepaper, arXiv:1308.3468 [hep-ph].
[18] G.D. Kribs, E. Poppitz, N. Weiner, Flavor in supersymmetry with an extended R-symmetry, Phys. Rev. D 78 (2008) 055010, arXiv:0712.2039 [hep-ph].
[19] R. Fok, G.D. Kribs, μ to e in R-symmetric supersymmetry, Phys. Rev. D 82 (2010) 035010, arXiv:1004.0556 [hep-ph].
[20] E. Dudas, M. Goodsell, L. Heurtier, P. Tziveloglou, Flavour models with Dirac and fake gluinos, Nucl. Phys. B 884 (2014) 632–671, arXiv:1312.2011 [hep-ph].
[21] G. Belanger, K. Benakli, M. Goodsell, C. Moura, A. Pukhov, Dark matter with Dirac and Majorana gaugino masses, J. Cosmol. Astropart. Phys. 0908 (2009) 027, arXiv:0905.1043 [hep-ph].
[22] K. Benakli, M.D. Goodsell, A.-K. Maier, Generating μ and $B\mu$ in models with Dirac gauginos, Nucl. Phys. B 851 (2011) 445–461, arXiv:1104.2695 [hep-ph].
[23] K. Benakli, M.D. Goodsell, F. Staub, Dirac gauginos and the 125 GeV Higgs, J. High Energy Phys. 06 (2013) 073, arXiv:1211.0552 [hep-ph].
[24] E. Bertuzzo, C. Frugiuele, T. Gregoire, E. Ponton, Dirac gauginos, R symmetry and the 125 GeV Higgs, J. High Energy Phys. 04 (2015) 089, arXiv:1402.5432 [hep-ph].
[25] P. Dießner, J. Kalinowski, W. Kotlarski, D. Stöckinger, Higgs boson mass and electroweak observables in the MRSSM, J. High Energy Phys. 12 (2014) 124, arXiv:1410.4791 [hep-ph].
[26] P. Diessner, J. Kalinowski, W. Kotlarski, D. Stöckinger, Two-loop correction to the Higgs boson mass in the MRSSM, Adv. High Energy Phys. 2015 (2015) 760729, arXiv:1504.05386 [hep-ph].
[27] J. Polchinski, L. Susskind, Breaking of supersymmetry at intermediate-energy, Phys. Rev. D 26 (1982) 3661.
[28] L.J. Hall, L. Randall, $U(1)_R$ symmetric supersymmetry, Nucl. Phys. B 352 (1991) 289–308.
[29] A.E. Nelson, N. Rius, V. Sanz, M. Unsal, The minimal supersymmetric model without a mu term, J. High Energy Phys. 08 (2002) 039, arXiv:hep-ph/0206102.
[30] I. Antoniadis, K. Benakli, A. Delgado, M. Quiros, A new gauge mediation theory, Adv. Stud. Theor. Phys. 2 (2008) 645–672, arXiv:hep-ph/0610265.
[31] S.D.L. Amigo, A.E. Blechman, P.J. Fox, E. Poppitz, R-symmetric gauge mediation, J. High Energy Phys. 01 (2009) 018, arXiv:0809.1112 [hep-ph].
[32] T. Plehn, T.M.P. Tait, Seeking sgluons, J. Phys. G 36 (2009) 075001, arXiv:0810.3919 [hep-ph].
[33] K. Benakli, M.D. Goodsell, Dirac gauginos in general gauge mediation, Nucl. Phys. B 816 (2009) 185–203, arXiv:0811.4409 [hep-ph].
[34] K. Benakli, M.D. Goodsell, Dirac gauginos and kinetic mixing, Nucl. Phys. B 830 (2010) 315–329, arXiv:0909.0017 [hep-ph].
[35] S.Y. Choi, J. Kalinowski, J.M. Kim, E. Popenda, Scalar gluons and Dirac gluinos at the LHC, Acta Phys. Pol. B 40 (2009) 2913–2922, arXiv:0911.1951 [hep-ph].
[36] K. Benakli, M.D. Goodsell, Dirac gauginos, gauge mediation and unification, Nucl. Phys. B 840 (2010) 1–28, arXiv:1003.4957 [hep-ph].
[37] S.Y. Choi, D. Choudhury, A. Freitas, J. Kalinowski, J.M. Kim, P.M. Zerwas, Dirac neutralinos and electroweak scalar bosons of $N = 1/N = 2$ hybrid supersymmetry at colliders, J. High Energy Phys. 08 (2010) 025, arXiv:1005.0818 [hep-ph].
[38] L.M. Carpenter, Dirac gauginos, negative supertraces and gauge mediation, J. High Energy Phys. 09 (2012) 102, arXiv:1007.0017 [hep-th].

[39] G.D. Kribs, T. Okui, T.S. Roy, Viable gravity-mediated supersymmetry breaking, Phys. Rev. D 82 (2010) 115010, arXiv:1008.1798 [hep-ph].
[40] S. Abel, M. Goodsell, Easy Dirac gauginos, J. High Energy Phys. 06 (2011) 064, arXiv:1102.0014 [hep-th].
[41] R. Davies, J. March-Russell, M. McCullough, A supersymmetric one Higgs doublet model, J. High Energy Phys. 1104 (2011) 108, arXiv:1103.1647 [hep-ph].
[42] J. Kalinowski, Phenomenology of R-symmetric supersymmetry, Acta Phys. Pol. B 42 (2011) 2425–2432.
[43] C. Frugiuele, T. Gregoire, Making the sneutrino a Higgs with a $U(1)_R$ lepton number, Phys. Rev. D 85 (2012) 015016, arXiv:1107.4634 [hep-ph].
[44] E. Bertuzzo, C. Frugiuele, Fitting neutrino physics with a $U(1)_R$ lepton number, J. High Energy Phys. 1205 (2012) 100, arXiv:1203.5340 [hep-ph].
[45] R. Davies, Dirac gauginos and unification in F-theory, J. High Energy Phys. 1210 (2012) 010, arXiv:1205.1942 [hep-th].
[46] R. Argurio, M. Bertolini, L. Di Pietro, F. Porri, D. Redigolo, Holographic correlators for general gauge mediation, J. High Energy Phys. 1208 (2012) 086, arXiv:1205.4709 [hep-th].
[47] R. Argurio, M. Bertolini, L. Di Pietro, F. Porri, D. Redigolo, Exploring holographic general gauge mediation, J. High Energy Phys. 1210 (2012) 179, arXiv:1208.3615 [hep-th].
[48] C. Frugiuele, T. Gregoire, P. Kumar, E. Ponton, '$L = R$' – $U(1)_R$ as the origin of leptonic 'RPV', J. High Energy Phys. 1303 (2013) 156, arXiv:1210.0541 [hep-ph].
[49] C. Frugiuele, T. Gregoire, P. Kumar, E. Ponton, '$L = R$' – $U(1)_R$ lepton number at the LHC, J. High Energy Phys. 1305 (2013) 012, arXiv:1210.5257 [hep-ph].
[50] H. Itoyama, N. Maru, D-term triggered dynamical supersymmetry breaking, Phys. Rev. D 88 (2013) 025012, arXiv:1301.7548 [hep-ph].
[51] S. Chakraborty, S. Roy, Higgs boson mass, neutrino masses and mixing and keV dark matter in an $U(1)_R$-lepton number model, J. High Energy Phys. 1401 (2014) 101, arXiv:1309.6538 [hep-ph].
[52] C. Csaki, J. Goodman, R. Pavesi, Y. Shirman, The m_D–b_M problem of Dirac gauginos and its solutions, Phys. Rev. D 89 (5) (2014) 055005, arXiv:1310.4504 [hep-ph].
[53] H. Itoyama, N. Maru, 126 GeV Higgs boson associated with D-term triggered dynamical supersymmetry breaking, Symmetry 7 (1) (2015) 193–205, arXiv:1312.4157 [hep-ph].
[54] H. Beauchesne, T. Gregoire, Electroweak precision measurements in supersymmetric models with a $U(1)_R$ lepton number, J. High Energy Phys. 05 (2014) 051, arXiv:1402.5403 [hep-ph].
[55] M.D. Goodsell, P. Tziveloglou, Dirac gauginos in low scale supersymmetry breaking, Nucl. Phys. B 889 (2014) 650–675, arXiv:1407.5076 [hep-ph].
[56] D. Busbridge, Constrained Dirac gluino mediation, arXiv:1408.4605 [hep-ph].
[57] S. Chakraborty, A. Datta, S. Roy, $h\to\gamma\gamma$ in $U(1)_R$-lepton number model with a right-handed neutrino, J. High Energy Phys. 02 (2015) 124, arXiv:1411.1525 [hep-ph];
S. Chakraborty, A. Datta, S. Roy, $h\to\gamma\gamma$ in $U(1)_R$-lepton number model with a right-handed neutrino, J. High Energy Phys. 09 (2015) 077, Erratum.
[58] R. Ding, T. Li, F. Staub, C. Tian, B. Zhu, Supersymmetric standard models with a pseudo-Dirac gluino from hybrid F- and D-term supersymmetry breaking, Phys. Rev. D 92 (1) (2015) 015008, arXiv:1502.03614 [hep-ph].
[59] D.S.M. Alves, J. Galloway, M. McCullough, N. Weiner, Goldstone gauginos, Phys. Rev. Lett. 115 (16) (2015) 161801, arXiv:1502.03819 [hep-ph].
[60] D.S.M. Alves, J. Galloway, M. McCullough, N. Weiner, Models of goldstone gauginos, Phys. Rev. D 93 (7) (2016) 075021, arXiv:1502.05055 [hep-ph].
[61] L.M. Carpenter, J. Goodman, New calculations in Dirac gaugino models: operators, expansions, and effects, J. High Energy Phys. 07 (2015) 107, arXiv:1501.05653 [hep-ph].
[62] S.P. Martin, Nonstandard supersymmetry breaking and Dirac gaugino masses without supersoftness, Phys. Rev. D 92 (3) (2015) 035004, arXiv:1506.02105 [hep-ph].
[63] P. Diessner, J. Kalinowski, W. Kotlarski, D. Stöckinger, Exploring the Higgs sector of the MRSSM with a light scalar, J. High Energy Phys. 03 (2016) 007, arXiv:1511.09334 [hep-ph].
[64] K. Benakli, Dirac gauginos: a user manual, Fortschr. Phys. 59 (2011) 1079–1082, arXiv:1106.1649 [hep-ph].
[65] K. Benakli, L. Darmé, M.D. Goodsell, P. Slavich, A fake split supersymmetry model for the 126 GeV Higgs, J. High Energy Phys. 05 (2014) 113, arXiv:1312.5220 [hep-ph].
[66] F. Staub, SARAH, arXiv:0806.0538 [hep-ph].
[67] F. Staub, From superpotential to model files for FeynArts and CalcHep/CompHep, Comput. Phys. Commun. 181 (2010) 1077–1086, arXiv:0909.2863 [hep-ph].
[68] F. Staub, Automatic calculation of supersymmetric renormalization group equations and self energies, Comput. Phys. Commun. 182 (2011) 808–833, arXiv:1002.0840 [hep-ph].

[69] F. Staub, SARAH 3.2: Dirac gauginos, UFO output, and more, Comput. Phys. Commun. 184 (2013) 1792–1809, arXiv:1207.0906 [hep-ph].
[70] F. Staub, SARAH 4: a tool for (not only SUSY) model builders, Comput. Phys. Commun. 185 (2014) 1773–1790, arXiv:1309.7223 [hep-ph].
[71] F. Staub, Exploring new models in all detail with SARAH, Adv. High Energy Phys. 2015 (2015) 840780, arXiv:1503.04200 [hep-ph].
[72] W. Porod, SPheno, a program for calculating supersymmetric spectra, SUSY particle decays and SUSY particle production at e+ e- colliders, Comput. Phys. Commun. 153 (2003) 275–315, arXiv:hep-ph/0301101.
[73] W. Porod, F. Staub, SPheno 3.1: extensions including flavour, CP-phases and models beyond the MSSM, Comput. Phys. Commun. 183 (2012) 2458–2469, arXiv:1104.1573 [hep-ph].
[74] M.D. Goodsell, K. Nickel, F. Staub, Two-loop Higgs mass calculations in supersymmetric models beyond the MSSM with SARAH and SPheno, Eur. Phys. J. C 75 (1) (2015) 32, arXiv:1411.0675 [hep-ph].
[75] M. Goodsell, K. Nickel, F. Staub, Generic two-loop Higgs mass calculation from a diagrammatic approach, Eur. Phys. J. C 75 (6) (2015) 290, arXiv:1503.03098 [hep-ph].
[76] M.D. Goodsell, F. Staub, The Higgs mass in the CP violating MSSM, NMSSM, and beyond, arXiv:1604.05335 [hep-ph].
[77] M.D. Goodsell, Two-loop RGEs with Dirac gaugino masses, J. High Energy Phys. 01 (2013) 066, arXiv:1206.6697 [hep-ph].
[78] L.M. Carpenter, R. Colburn, J. Goodman, Supersoft SUSY models and the 750 GeV diphoton excess, beyond effective operators, arXiv:1512.06107 [hep-ph].
[79] S. Chakraborty, A. Chakraborty, S. Raychaudhuri, Diphoton resonance at 750 GeV in the broken MRSSM, arXiv:1512.07527 [hep-ph].
[80] T. Cohen, G.D. Kribs, A.E. Nelson, B. Ostdiek, 750 GeV diphotons from supersymmetry with Dirac gauginos, arXiv:1605.04308 [hep-ph].
[81] R. Franceschini, G.F. Giudice, J.F. Kamenik, M. McCullough, A. Pomarol, R. Rattazzi, M. Redi, F. Riva, A. Strumia, R. Torre, What is the $\gamma\gamma$ resonance at 750 GeV?, J. High Energy Phys. 03 (2016) 144, arXiv:1512.04933 [hep-ph].
[82] C. Petersson, R. Torre, 750 GeV diphoton excess from the Goldstino superpartner, Phys. Rev. Lett. 116 (15) (2016) 151804, arXiv:1512.05333 [hep-ph].
[83] J.A. Casas, J.R. Espinosa, J.M. Moreno, The 750 GeV diphoton excess as a first light on supersymmetry breaking, Phys. Lett. B 759 (2016) 159–165, arXiv:1512.07895 [hep-ph].
[84] Q.-H. Cao, Y.-Q. Gong, X. Wang, B. Yan, L.L. Yang, One bump or two peaks: the 750 GeV diphoton excess and dark matter with a complex mediator, Phys. Rev. D 93 (7) (2016) 075034, arXiv:1601.06374 [hep-ph].
[85] G. Belanger, K. Benakli, M. Goodsell, C. Moura, A. Pukhov, Dark matter with Dirac and Majorana gaugino masses, J. Cosmol. Astropart. Phys. 0908 (2009) 027.
[86] T. Gherghetta, A. Pomarol, A distorted MSSM Higgs sector from low-scale strong dynamics, J. High Energy Phys. 12 (2011) 069, arXiv:1107.4697 [hep-ph].
[87] P.J. Fox, A.E. Nelson, N. Weiner, Dirac gaugino masses and supersoft supersymmetry breaking, J. High Energy Phys. 08 (2002) 035, arXiv:hep-ph/0206096.
[88] M.D. Goodsell, Two-loop RGEs with Dirac gaugino masses, J. High Energy Phys. 1301 (2013) 066.
[89] ATLAS Collaboration, CMS Collaboration, Measurements of the Higgs boson production and decay rates and constraints on its couplings from a combined ATLAS and CMS analysis of the LHC, pp collision data at $\sqrt{s} =$ 7 and 8 TeV, arXiv:1606.02266 [hep-ex].
[90] A search for resonant Higgs-pair production in the $b\bar{b}b\bar{b}$ final state in pp collisions at $\sqrt{s} = 8$ TeV, Tech. Rep. ATLAS-CONF-2014-005. CERN, Geneva, Mar 2014, http://cds.cern.ch/record/1666518.
[91] ATLAS Collaboration, G. Aad, et al., Search for an additional, heavy Higgs boson in the $H \to ZZ$ decay channel at $\sqrt{s} = 8$ TeV in pp collision data with the ATLAS detector, Eur. Phys. J. C 76 (1) (2016) 45, arXiv:1507.05930 [hep-ex].
[92] ATLAS Collaboration, G. Aad, et al., Search for a CP-odd Higgs boson decaying to Zh in pp collisions at $\sqrt{s} =$ 8 TeV with the ATLAS detector, Phys. Lett. B 744 (2015) 163–183, arXiv:1502.04478 [hep-ex].
[93] CMS Collaboration, V. Khachatryan, et al., Search for a Higgs boson in the mass range from 145 to 1000 GeV decaying to a pair of W or Z bosons, J. High Energy Phys. 10 (2015) 144, arXiv:1504.00936 [hep-ex].
[94] ATLAS Collaboration, G. Aad, et al., Search for a high-mass Higgs boson decaying to a W boson pair in pp collisions at $\sqrt{s} = 8$ TeV with the ATLAS detector, J. High Energy Phys. 01 (2016) 032, arXiv:1509.00389 [hep-ex].
[95] S.Y. Choi, M. Drees, J. Kalinowski, J.M. Kim, E. Popenda, P.M. Zerwas, Color-octet scalars of $N = 2$ supersymmetry at the LHC, Phys. Lett. B 672 (2009) 246–252, arXiv:0812.3586 [hep-ph].
[96] CMS Collaboration, S. Chatrchyan, et al., Searches for new physics using the $t\bar{t}$ invariant mass distribution in pp collisions at $\sqrt{s} = 8$ TeV, Phys. Rev. Lett. 111 (21) (2013) 211804, arXiv:1309.2030;

CMS Collaboration, S. Chatrchyan, et al., Searches for new physics using the $t\bar{t}$ invariant mass distribution in pp collisions at $\sqrt{s} = 8$ TeV, Phys. Rev. Lett. 112 (11) (2014) 119903, Erratum.

[97] CMS Collaboration, V. Khachatryan, et al., Search for standard model production of four top quarks in the lepton + jets channel in pp collisions at $\sqrt{s} = 8$ TeV, J. High Energy Phys. 11 (2014) 154, arXiv:1409.7339 [hep-ex].

[98] ATLAS Collaboration, Search for production of vector-like top quark pairs and of four top quarks in the lepton-plus-jets final state in pp collisions at $\sqrt{s} = 13$ TeV with the ATLAS detector, arXiv:1505.04306 [hep-ex].

[99] L. Beck, F. Blekman, D. Dobur, B. Fuks, J. Keaveney, K. Mawatari, Probing top-philic sgluons with LHC Run I data, Phys. Lett. B 746 (2015) 48–52, arXiv:1501.07580 [hep-ph].